SU-SEL-72-019

# COPY

VHF/UHF Technique for the Determination of the Columnar Electron Contents of the Plasmasphere and of the Protonosphere Using Geostationary Satellite Transmissions: Observations during Magnetic Storms

by

Odmar Geraldo Almeida

May 1972

Technical Report No. 14

Prepared under

National Aeronautics and Space Administration Research Grant No. 05-020-001

RADIOSCIENCE LABORATORY

STANFORD ELECTRONICS LABORATORIES

STANFORD UNIVERSITY · STANFORD, CALIFORNIA



VHF/UHF TECHNIQUE FOR THE DETERMINATION
OF THE COLUMNAR ELECTRON CONTENTS
OF THE PLASMASPHERE AND OF THE PROTONOSPHERE
USING GEOSTATIONARY SATELLITE TRANSMISSIONS:
OBSERVATIONS DURING MAGNETIC STORMS

by

Odmar Geraldo Almeida

May 1972

Technical Report No. 14

Prepared under

National Aeronautics and Space Administration Research Grant No. NGR 05-020-001

Radioscience Laboratory
Stanford Electronics Laboratories
Stanford University Stanford, California

#### ABSTRACT

Measurements of the 'total electron content' of the plasmasphere up to geostationary heights have been made using the beacon transmitters aboard the satellite ATS-3. The technique employed is a combination of the phase-path length difference and the Faraday rotation angle methods. Such a combination permits very accurate determination of the integration constant necessary to convert phase-path length difference data into information about the absolute value of the columnar content. In previous efforts, to combine both data to determine the columnar electron content of the upper plasmasphere (protonosphere), it was assumed that the Faraday rotation angle was a measure of electron content below a well-defined altitude so that the difference  $I_{m}$  between the 'total content' and the 'Faraday content' is the content above that altitude. In this work a more realistic interpretation of  $\mathbf{I}_{\mathbf{w}}$  is offered. It is demonstrated that  $\mathbf{I}_{\mathbf{w}}$  is a useful information of the protonospheric content under certain geometries of observation, such as Stanford and the geostationary satellite parked at -73° E. For such geometry, if diffusive equilibrium models of the ionization field-line distribution are valid approximations,  $\mathbf{I}_{_{\mathbf{W}}}$  is a good measure of the protonospheric electron content above approximately 2300 km. The data taken at Stanford using ATS-3 satellite are presented and interpreted in terms of changes in electron content of the upper plasmasphere. The data during the storm of 14 May 1969 show a sudden increase in I  $_{\rm w}$  immediately following the SSC at 1929 UT (1430 LT at ATS-3). The increase lasts for some three hours, and then  $I_{_{\rm IV}}$  decreases below the average level, followed by a slow recovery for several days. This behavior is consistent with a storm model in which the outer plasmasphere is 'peeled' away by sunward convection and is subsequently replenished by slow filling from the underlying ionosphere. The estimated intensity of the east-west component of the electric field associated with this peeling process is of the order of  $1 \text{ mV.m}^{-1}$ .

#### **ACKNOWLEDGEMENTS**

I am very grateful to Dr. A.V. da Rosa for his invaluable guidance and encouragement throughout the course of this work, and to Professor O.K. Garriott for suggesting the experiment. I wish to thank Dr. C.G. Park for the enlightening discussions on interpretation of the results. I have benefitted from discussions with Dr. M.J. Davis and Dr. H. Waldman.

The constant support and attention of the ATS-Project Office (NASA Goddard Space Flight Center) is appreciated.

This research was supported by NASA Research Grant No. NGR 05-020-001.

# TABLE of CONTENTS

_		Page
I.	INTRODUCTION	1
	A. Faraday Polarization Changes and Phase-path Length	
	Effects	5
II.	DETERMINATION OF THE COLUMNAR ELECTRON CONTENT AND THE PARAMETER G OF THE PLASMASPHERE UP TO GEOSTATIONARY	
	HEIGHTS	13
	A. The Experiment	14
	B. Data Reduction	15
	C. Determination of the Absolute Value of Total	
	Columnar Electron Content	20
	MEGINITATIE OF PROMONOGRIFFITO DI ECURONI COMMENTO	
III.	TECHNIQUE OF PROTONOSPHERIC ELECTRON CONTENT DETERMINATION USING GEOSTATIONARY SATELLITE	35
	A. Analysis	36
	B. Geostationary Satellite Observations Combined with	
	Backscatter Ionization Profiles	53
IV.	RESULTS	57
	A. Arecibo Observations	58
	D. Stanford Observations During the Magnetic Disturbed	
	B. Stanford Observations During the Magnetic Disturbed Period of 12 to 18 May 1969	62
	C. Protonospheric Content Observations During Magnetic	
	Storms	68
v.	CONCLUSIONS	79
	REFERENCES	95

# TABLES

Number		Page
1	Comparison Between the Form Factors, Go	
	Calculated Independently and the Factor,	
	G, Obtained from the Least Error Analysis	. 32

## ILLUSTRATIONS

Figure		Page
1	Actual Spectrum of the UHF Signal Radiated by ATS-3	16
2	Retouched Photograph of the Differential Doppler Fringes	17
3a,b	Example of Plots of the Ratio Between the Quantities $\Delta\Omega=(\Omega-\Omega)$ and I = (I - I ref) Used to Estimate Values of the Parameter G	23
3c,d e,f	Example of Plots of $\Delta\Omega/\Delta I$ for Arecibo, 06 December 1968 at 1420 AST	24
4	Diurnal Variation of the Total Slant Electron Content I, and of the Parameter G, for Several Days in December 1968	27
5	Diurnal Variation of the Total Electron Content of the Plasmasphere	31
6	Plots of the Weight Function W Versus Height for an Observer at Stanford	40
7	Plots of the Weight Function W Versus Height for an Observer at Arecibo	41
8	Contribution of the Ionospheric Region to I for Stanford and a Geostationary Satellite at -73° E	44
9	Contribution of the Ionospheric Region to I for Arecibo and a Geostationary Satellite at $-73^{\circ}$ E	45
10	Comparison Between Computed Ionospheric Contributions to I $_{\rm W}$ for Arecibo and a Geostationary satellite at -73°E	47
11 .	Plot of the Maximum Computed Fluctuation of Ionospheric Contribution to I, for Stanford, Versus Satellite Longitude	48
12	Variation with Height of the Ratio Between the Quantity I and the Electron Content Above that Height for Stanford and a Geostationary Satellite at -73° E	51
13	Plots of Total Slant Electron Content, I, and of the Quantities I Determined from Observations of ATS-3 at Arecibo	60
14	Diurnal Variation of Protonospheric Electron Content at Arecibo	61

# ILLUSTRATIONS (cont.)

Figure		Page
15	Protonospheric Electron Content Observation, During an Uninterrupted Period of 7 Days in May 1969, from	
	Stanford	64
16	Protonospheric Electron Content on 14 May 1969, from	
-	Stanford	71
17	Qualitative Picture of the Shape of the Plasmapause	
	Trace on the Earth's Equatorial Plane	73

#### LIST OF SYMBOLS

```
AST = Antilles Standard Time, defined as: UT - 4 hours
B = magnitude of the geomagnetic flux density (page 6)
B_0 = value of B on the Earth's surface (page 76)
B_{T} = B \cos \theta = \text{component along the path of propagation of the geomagnetic}
     flux density (page 8)
B_{T,T} = value of B_{T} computed at heights around 300 km (page 37)
\langle B_{1} \rangle = mean longitudinal geomagnetic flux density (page 9)
c = speed of light in free space (page 7)
D = geometric distance (page 7)
e = electron charge (page 6)
E = East
E = electric field (page 74)
E_{co} = \text{east-west} component of the electric field (page 75)
f = wave frequency (page 6)
f<sub>b</sub> = beat frequency (pages 14 and 18)
f_{\tau} = ionospheric Doppler frequency shift (page 10)
f_{g} = spin frequency of the satellite (page 15)
f<sub>IHF(R)</sub> = received UHF frequency (page 15)
f = vaccum Doppler frequency shift (page 15)
f_{VHF(R)} = received VHF frequency (page 15)
f<sub>VHF(T)</sub> = transmitted VHF frequency (page 15)
G = ratio between Faraday rotation angle and columnar electron content
    (page 9)
G_T = value of G computed at heights around 300 km (page 35)
h = altitude
h_{max} = altitude of the electron concentration peak of F_2 layer (page 46)
```

I = slant columnar electron content (page 8)

I = time derivative of I

 $L_{p} = \Omega/GI$  (page 35)

 $I_{\ell}$  = electron content associated with the ionospheric ionization profile (page 43)

 $I_{T}$  = electron content of a tube of force from 1000 km to the equatorial plane

 $I_u = \text{columnar electron content of the region extending from altitude h}$  to 4 Earth radii (page 50)

 $I_{w} = I - \Omega/G_{\tau}$  (pages 36 and 37)

 $I_{w\ell} = \int_{0}^{800} nW \sec \chi \, dh, h \text{ in km (page 42)}$ 

 $I_{wi} = \int_{800}^{10,000} \text{nW sec } \chi \text{ dh, h in km (page 49)}$ 

 $I_{wu} = \int_{10,000}^{35,600} \text{nW sec } \chi \text{ dh, h in km (page 49)}$ 

 $K_{p}$  = three hour universal geomagnetic index

L = value of the L-shell parameter

 $L_{p}$  = value of L at the plasmapause

LT = Local Time

m = electron mass (page 6)

n = electron concentration (page 6)

P = phase-path length (page 7)

PST = Pacific Standard Time, defined as: UT - 8 hours

R = radius of the Earth (6,371.2 km)

t = time

UT = Universal Time

 $\overrightarrow{v}$  = plasma drift velocity (page 74)

 $W = (1 - B_L/B_{LI})$ 

 $X = \frac{80.6n}{e^2} \text{ (page 6)}$ 

SEL-72-019

$$Y = \frac{eB}{2\pi mf}$$
 (page 6)

$$Z = \frac{v}{2\pi f}$$
 (page 6)

 $\alpha$  = angle between the ray and the wave normal (page 7)

 $\Delta I$  = columnar electron content increment

 $\Delta I_n = \text{protonospheric electron content increment}$ 

 $\Delta I_w = increment in I_w$ 

 $\Delta P$  = phase-path length reduction (page 7)

 $\Delta t = time increment$ 

 $\Delta\Omega$  = Faraday rotation angle increment

 $\mathcal{E}_{0}$  = permittivity of free space (page 6)

 $\theta$  = angle between wave normal and magnetic field (page 6)

 $\lambda$  = free space wavelength (page 10)

 $\mu = refractive index (page 6)$ 

v = electron-neutral collision frequency (page 6)

 $\chi$  = satellite zenithal angle

 $\Omega$  = Faraday rotation angle (page 7)

#### CHAPTER I

#### INTRODUCTION

The purpose of this report is to describe a new technique of protonospheric measurements and discuss the results obtained from observations made during geomagnetic storms. The quantity measured is the columnar electron content of the protonosphere.

The protonosphere is the region of the Earth's atmosphere where the Hydrogen ions, H+, are the dominant ion species. This region extends from heights of 1500 km to several Earth radii (~20,000km) and it often terminates at a sharp geomagnetic field-aligned boundary, the plasmapause, where the charged particle concentration is reduced by 1 order of magnitude or more (Carpenter[1962][1966]). The region inside the plasmapause, the plasmaphere, has approximately the shape of a 'donut' and is essentially populated by low energy particles. In the region outside the plasmapause, the plasma trough, equatorial concentrations are typically 10 el.cm<sup>-3</sup> or less.

The detection of the plasmapause in the equatorial height distribution of electron density, obtained by the whistler technique, has been extensively used to study the behavior of that region. The position of the plasmapause depends on local time and geomagnetic activity. Under moderate geomagnetic activity the shape of the plasmapause trace on the Earth's equatorial plane is roughly circular with an average geocentric distance of 4 Earth radii, and exhibits a pronounced asymmetry in the dusk-midnight sector. At around 1800 LT (Local Time) there is a sharp increase in the geocentric distance of the plasmapause which moves from

approximately 3.5 to 5 Earth radii. This bulge region extends from about the 1800 LT to the 2100 LT meridians. After 2100 LT the height of the plasmapause decreases very slowly to 3.5 Earth radii at dawn. With increasing geomagnetic activity the plasmasphere envelope compresses and the asymmetry increases. During geomagnetically quiet periods the envelope expands and the asymmetry decreases. Such compression and expansion of the plasmasphere is reflected in the Earth equatorial plane by a corresponding inward or outward motion of the plasmapause trace, which resembles more a circle under very quiet magnetic conditions.

The study of the shape and general behavior of the plasmapause prompted Carpenter[1962], to suggest that the plasmapause might be identified with the inner boundary of the magnetospheric convection flow pattern proposed by Axford and Hines[1961].

It is now generally accepted that a convection electric field, probably of solar wind origin, causes the circulation of the geomagnetic field tubes in which the plasma is 'frozen in' (Axford[1969]). The high latitude tubes become open when convected through the polar cap and return through lower latitudes where they are closed again. The plasmapause is believed to be the boundary between flux tubes that corrotate with the Earth, remaining always closed and therefore holding their plasma, and flux tubes which are convected to the magnetopause where they lose their plasma.

Actually, in the dynamics of the plasmapause behavior the situation is a little more complicated because the convection field varies with magnetic activity and the ionization tubes are filled by the ionosphere on the dayside.

The study of the dynamics of the plasmapause has been mostly based on data provided by the whistler technique. More recently, direct measurements of ion concentration in the magnetosphere by light-ion mass spectrometer flown in high altitude satellites (c.f. <u>Taylor et al.</u>[1968], <u>Chappell et al.</u>[1970],[1971]) have been very useful in those investigations.

Determinations of the protonospheric electron content may bring more information on the remote magnetosphere. The possibility of using geostationary beacons for continuous observations of the protonospheric content, with excellent time resolution, makes such determinations more attractive.

Faraday rotation angle and phase-path difference data observed using VHF and UHF transmissions from geostationary satellites, under certain geometries of observation, can provide the necessary information for protonospheric electron content determination, as will be demonstrated in Chapter 3.

The Faraday polarization changes and phase-path length reduction effects, briefly discussed in the next Section, reflect the electron content of both the ionosphere and protonosphere regions traversed by the radio signals. The phase-path difference data is equally sensitive to ionization changes at any height along the path of propagation. The Faraday effect, on the other hand, is more sensitive to ionization changes at lower heights, because it is related to the product of the electron concentration by the component along the path of propagation (longitudinal component), B<sub>L</sub>, of the geomagnetic field. Consequently, the protonospheric information can be separated, in principle, from the ionospheric content

by combining both data.

One of the difficulties encountered lies in the fact that the protonosphere accounts for a relatively small fraction of the total information in the data, of the order of 10%. Therefore, very accurate determinations of the total electron content must be made in order to achieve reasonably good determinations of protonospheric content.

Almeida et al.[1970], have proposed a very accurate method of total electron content determination by combining the Faraday and phase-path difference data. Such method, in spite of being rigorously correct, is of very difficult application because it is based on the determination of a parameter G, the layer shape factor, using the time derivatives of the Faraday rotation angle and the phase-path length when the shape and height of the ionization profile is not changing with time. Although such moments do exist, they occur in general at moments when the data are slowly changing with time. This behavior combined with the noise level enhancement effect of the differentiation operation may cause a severe deterioration in the accuracy of determination of the mentioned parameter.

A new method of determination of the parameter G, and of the total electron content in which the above difficulties are avoided, is proposed in Chapter 2. The accuracy achieved by this new method is consistent with good protonospheric content determinations.

A critical analysis of the quantity  $I_w$ , resulting from the combination of the Faraday rotation angle and the phase-path difference data, is presented in Chapter 3. It will be demonstrated that for some geometries of observation the contribution of the ionospheric content to  $I_w$  can be minimized to a degree low enough not to mask the protonospheric informa-

tion. For such geometries, the interpretation of the meaning of  $I_w$  in terms of the columnar electron content of the protonosphere will be discussed based on diffusive equilibrium models of the field-line ionization distribution (Angerami[1966]).

Protonospheric observations made at Arecibo and at Stanford, using the new technique developed in the present work, will be presented in Chapter 4.

# A. Faraday polarization changes and phase-path length reduction effects.

It is well known that the polarization and phase path length of a radio wave may be affected by its propagation through the ionosphere.

Many authors have discussed the theoretical development of the equations relating the polarization plane rotation angle (Faraday rotation angle) and the phase-path length reduction to the columnar electron content of the ionosphere. (c.f. Browne et al.[1956], Ross[1965], Garriott et al. [1970]). A recapitulation is presented here for the sake of completeness.

In a medium such as the ionosphere characterized by the existence of free electrons and containing a static magnetic field, circularly polarized electromagnetic waves propagating along the magnetic field direction will not suffer change in polarization. Such waves, as shown by Lorentz [1906], are characteristic waves of that medium. For propagation paths not aligned with the magnetic field the characteristic waves are very approximately circularly polarized, provided the direction of propagation does not come too close to the normal to the magnetic field, a condition called "quasi-longitudinal (QL)". Under the QL approximation two waves with nearly circular polarization and sense of rotation opposite to one another propagate without changes in polarization. The refractive indexes,

μ, for these two waves under the QL assumption, are given by

$$\mu^2 = 1 - \frac{X}{1 \pm Y \cos \theta - iZ} \tag{1}$$

where .

$$X = \frac{ne^2}{4\pi^2 \ell_0 mf^2} = 80.6 \frac{n}{f^2}$$

$$Y = \frac{eB}{2\pi m f}$$

$$\mathbf{Z} = \frac{\mathbf{v}}{2\pi\mathbf{f}}$$

 $\boldsymbol{\theta}$  = angle between wave normal and magnetic field

 $v = electron-neutral collision frequency in sec^{-1}$ 

 $f = wave frequency in sec^{-1}$ 

e = electron charge in coulombs

m = electron mass in kilograms

n = electron concentration in m

 $\mathcal{E}_{0}$  = permittivity of free space in farads m<sup>-1</sup>

 $B = magnetic flux density in Wb m^{-2}$ 

The QL approximation is valid and therefore the given form of the refractive index holds true (see Ratcliffe[1959]), if

$$\frac{(Y \sin \theta)^4}{(2Y \cos \theta)^2} \ll \left| (1-X-iZ)^2 \right|$$

The plus and minus signs in Equation (1) refer to each of the two possible modes of propagation. The phase path length, P, for any one of the modes is given (see <a href="Budden">Budden</a>[1961]) by

$$P = \int \mu \cos \alpha \, ds \tag{2}$$

where  $\alpha$  is the angle between the ray and the wave normal, and the integral is taken along the ray path.

The phase path length reduction,  $\Delta P$ , is, by definition, the difference between the geometric distance, D, and the phase path length, P, both quantities taken for the same end points on the ray path.

$$\Delta P = D - P \tag{3}$$

Any wave other than the characteristic waves, when propagating in the ionosphere, will be split into the two modes, each propagating with its own characteristic phase velocity determined by the corresponding value of  $\mu$  given by Equation (1). At any point along the path of propagation the resultant polarization will be the combination of the two modes and it changes as the wave progresses along the path. The above described phenomenum is the well known Faraday rotation effect.

In the case of linear polarized waves propagating in the ionosphere under QL condition, the angular rotation,  $\Omega$ , of the polarization plane can be related to the differential phase shift between the two circularly polarized characteristic modes.

$$\Omega = \frac{\pi f}{c} \left( \Delta P_{-} - \Delta P_{+} \right) \tag{4}$$

The phase path length reductions  $\Delta P_{+}$  and  $\Delta P_{-}$  correspond respectively to the plus and minus signs of Equation (1).

The expression for  $\Omega$  in Equation (4) becomes quite simple in the case of waves of sufficiently high frequency for the refraction effects to become negligible; the ray path can then be approximated by a straight line path and  $\mu$  can be represented by the first order terms of its binomial expansion.

$$\mu = 1 - \frac{1}{2} (X \pm XY \cos \theta)$$
 (5)

For the high frequency approximation Z=0 and  $\cos\alpha=1$ , the expression for  $\Omega$  is then given by

$$\Omega = \frac{\pi f}{c} \int_{0}^{S} XY \cos\theta ds = \frac{2.36 \times 10^{4}}{f^{2}} \int_{0}^{S} nB \cos\theta ds$$
 (6)

Equation (6) shows clearly that the Faraday rotation angle is not related directly to the columnar electron content along the ray path,  $I = \int\!\! n ds, \text{ but to a content weighted by the longitudinal component of the local magnetic field, } B_I = B cos \theta.$ 

To obtain columnar electron content values from Faraday rotation angle measurements one must know the magnetic field and the shape of the profile of electron concentration all the way along the ray path. In the case of the ionosphere very good estimates of the geomagnetic field can be obtained from a spherical harmonic expansion, using the coefficients calculated by Jensen and Cain[1962], or the more recent ones of Cain and Sweeney[1970]. An electron concentration profile must be assumed based on theoretical models. The accuracy of columnar electron content values derived from Faraday rotation angle is thus very dependent upon one's ability of best guessing the proper electron concentration profile model to be used under the measurement circumstances.

It is usual to write Equation (6) in a form such that the Faraday rotation angle  $\Omega$  appears to be directly proportional to the columnar electron content I by defining the weighted mean value  $\langle B_L \rangle$  over the integration along the path between source and receiver. The 'mean longitudinal geomagnetic flux density' is, by definition, given by

$$\langle B_{L} \rangle = \frac{\int_{0}^{n} B_{L} ds}{\int_{0}^{n} n ds}$$
 (7)

It is convenient to define a parameter G as

$$G = \frac{2.36 \times 10^4}{f^2} \langle B_{\tilde{L}} \rangle \tag{8}$$

The parameter G defined by Equation (8) above, is a function of the frequency used and, of course, of the shape of electron concentration profile and the distribution of the longitudinal component of the geomagnetic flux density,  $B_L$ , along the path between source and receiver. It does not depend on the magnitude of the electron concentration.

Equation (6) can be rewritten as

$$\Omega = G I \tag{9}$$

Although it is convenient, and very often done, to relate the Faraday angle to the columnar electron content as in Equation (9), this does not necessarily mean that G is a constant factor which converts Faraday rotation angle data into electron content information. Even in the case of geostationary beacons where the B<sub>L</sub> distribution is stationary, fluctuations in the height and shape of the electron concentration profile throughout the day cause G not to be constant with time. The parameter G cannot be measured by using the Faraday data by itself, and is, therefore, usually only roughly estimated and often assumed to be time independent. Improvements on the estimated values of G can be realized by resorting to ancillary data such as electron concentration profiles from Thomson scatter observations,

(D.H. Smith[1970]), but such data are costly and can be obtained only in a few locations. However, even the best Thomson scatter data are limited in height; otherwise the total content could be determined from it alone. The maximum height of the scatter profiles can be made larger by increasing the integration time, but this sacrifices accuracy, because the electron distribution may change significantly during the observation interval. So, to calculate the total electron content from Faraday data combined with Thomson scatter information, there is always the necessity to extrapolate the profile shape beyond the maximum height of the Thomson data.

As pointed out in the beginning of this chapter, one of our contributions is the experimental determination of the parameter G and its diurnal variation.

A brief remark on the phase path length reduction will follow.

Under QL conditions of propagation and in the case of high-frequency waves, the phase path length reduction suffered by either mode of propagation is directly dependent on the columnar electron content along the ray path. The expression relating the phase path length reduction,  $\Delta P$ , to columnar electron content, I, is readily obtained by using Equations (2), (3), and (5).

$$\Delta P = \frac{40.3}{f^2} \int_0^S n \, ds \qquad (10)$$

The frequency shift seen at the receiver, the so-called ionospheric Doppler frequency shift, due only to changes in the amount of electrons along the transmitter-to-observer path is given by

$$f_{I} = \frac{1}{\lambda} \frac{d\Delta P}{dt} = \frac{40.3}{c} \frac{dI}{dt}$$
 (11)

where  $\lambda$  is the free space wavelength.

The cycle count of  $f_I$  yields values of columnar electron content increments  $\Delta I = (I - I_O)$  where  $I_O$  is the value of the electron content at the beginning of the count.

To obtain columnar electron content values from ionospheric Doppler frequency shifts one must know the absolute value of the columnar electron content at one given instant of time during the period of observation. At any other time t the columnar electron content will be given by

$$I = \frac{c}{40.3} \int_{t_0}^{t} f_1 dt + I_0$$

Methods for determination of the constant of integration I in the case of low orbit satellites have been discussed by several workers. In such cases, the determination of the unknown constant can be made by taking advantage of the fast angular motion of the spacecraft relative to the observer (de Mendonça[1962]). This clearly is not the case with geostationary beacons.

For such beacons a method of combining the Doppler frequency and the Faraday rotation angle measurements to determine the absolute value of the total columnar electron content was developed and is described in the present report.

Since geostationary radio beacons, orbiting at 6.6 Earth radii, are outside the plasmapause, except perhaps in geomagnetically very quiet days, (Carpenter[1966]), total columnar electron content values derived from ionospheric Doppler frequency shift data is a good measurement of the total electron content of the plasmapause.

#### CHAPTER II

DETERMINATION OF THE COLUMNAR ELECTRON CONTENT AND THE PARAMETER G OF THE PLASMASPHERE UP TO GEOSTATIONARY HEIGHTS.

The columnar electron content of the lower ionosphere, up to about 1000 km, has been measured by numerous authors using satellites in low altitude orbits. Good accuracies have been obtained from differential Doppler frequency observations (de Mendonça[1962]) or from a combination of differential Doppler frequency and Faraday rotation angle measurements (Garriott and de Mendonça[1963]). The columnar contents derived from the Faraday rotation angle only (Garriott[1960]) involve some uncertainty related to the unknown shape of the electron concentration profile. This drawback is of little importance in most applications; however, it becomes a major concern when the fine details of the plasmaspheric content changes are to be investigated.

The differential Doppler frequency, on the other hand, is equally sensitive to ionization changes at any altitude and provides a very accurate method of measuring the rate of change of columnar electron content. To obtain the absolute value of electron content at any time, it is necessary to integrate the observed rate of change and to determine the unknown integration constant from some additional information. This problem has been solved for the case of low orbiting satellites (c.f. Garriott, da Rosa, and Ross[1970]). It is the purpose of this section to describe a method for solving the same problem in the more difficult case of geostationary satellites by combining the differential Doppler frequency and the Faraday rotation angle measurements to determine the absolute value of the total plasmaspheric content.

### A. The Experiment

The experiment described in this report was carried out using VHF and UHF transmissions from the ATS-3 satellite. The 137.35 MHz VHF signal is the carrier of one of the regular telemetry transmitters while the 412.05 MHz UHF signal is the third harmonic of the VHF frequency, generated by a special multiplier installed aboard the satellite.

The effective radiated power (ERP) at VHF is about 2 W, which provides ample signal-to-noise ratios even when only a 12 dB antenna gain is used on the ground. The ERP at UHF is 12 mW but, due to the complicated spectrum of the signal resulting from the large spin modulation imparted by the rotation of the satellite, the ERP, in the dominant spectral component, is only 4.5 mW. In order to obtain good signal-to-noise ratios with the relatively modest antenna gain of 23 dB, great selectivity is necessary, so that only this dominant component is received. The bandwidth used is 1.5 Hz and the resulting signal-to-noise ratio is 19.4 dB. The use of a larger band-width in order to include more of the incoming UHF signal would actually decrease the signal-to-noise ratio.

The ground equipment performs the dual role of polarimeter for the VHF wave and of differential Doppler receiver using both the VHF and UHF signals. The outputs of this equipment consist of a) a voltage analog of the polarization angle ( $\Omega$ ) and b) the beat frequency ( $f_b$ ) between the selected component of the UHF spectrum and three times the VHF frequency. The polarimeter measures only angles between 0 and 180° so that a given number of half rotations have to be added to its reading. The resolution of this '180° ambiguity' has been discussed elsewhere (Smith III[1968]). The observed values of  $\Omega$  and  $f_b$  provide the data used in the analysis

described below.

## B. Data Reduction

If  $f_{VHF(T)}$  is the transmitted VHF frequency, then the received frequency will be

$$f_{VHF(R)} = f_{VHF(T)} + f_{I} + f_{V}$$
 (12)

where  $\mathbf{f}_{\mathbf{I}}$  is the frequency shift caused by changes in the intervening ionization and  $\mathbf{f}_{\mathbf{V}}$  is the vacuum Doppler shift due to the relative velocity between observer and satellite.

The carrier frequency of the transmitted UHF signal is exactly  $3f_{\mathrm{VHF}(T)}$ . The four antennas, which constitue the satellite transmitting array, are mounted on the rim of the spacecraft and are diametrically separated by a distance of 2 wavelengths. This arrangement results in a radiation pattern containing deep minima; consequently the spinning of the satellite causes a strong phase and amplitude modulation to be imposed on the carrier. This in turn creates numerous sidebands so that the complex spectrum shown in Figure 1 is actually emitted from the spacecraft. As can be seen from the figure, the dominant spectral line is the one with a frequency  $(3f_{\mathrm{VHF}(T)} - 2f_{\mathrm{S}})$ , where  $f_{\mathrm{S}}$  is the spin frequency of the satellite. The received UHF signal has a frequency

$$f_{UHF(R)} = 3f_{VHF(T)} - 2f_S + \frac{1}{3}f_I + 3f_V$$
 (13)

Here the effect of the ionization changes is only one third of that at VHF (neglecting very small higher order effects (Ross[1965]), while the vacuum Doppler shift is three times larger than at VHF.

The receiver performs the comparison between  $f_{UHF(R)}$  and three times  $f_{VHF(R)}$ , yielding a beat frequency

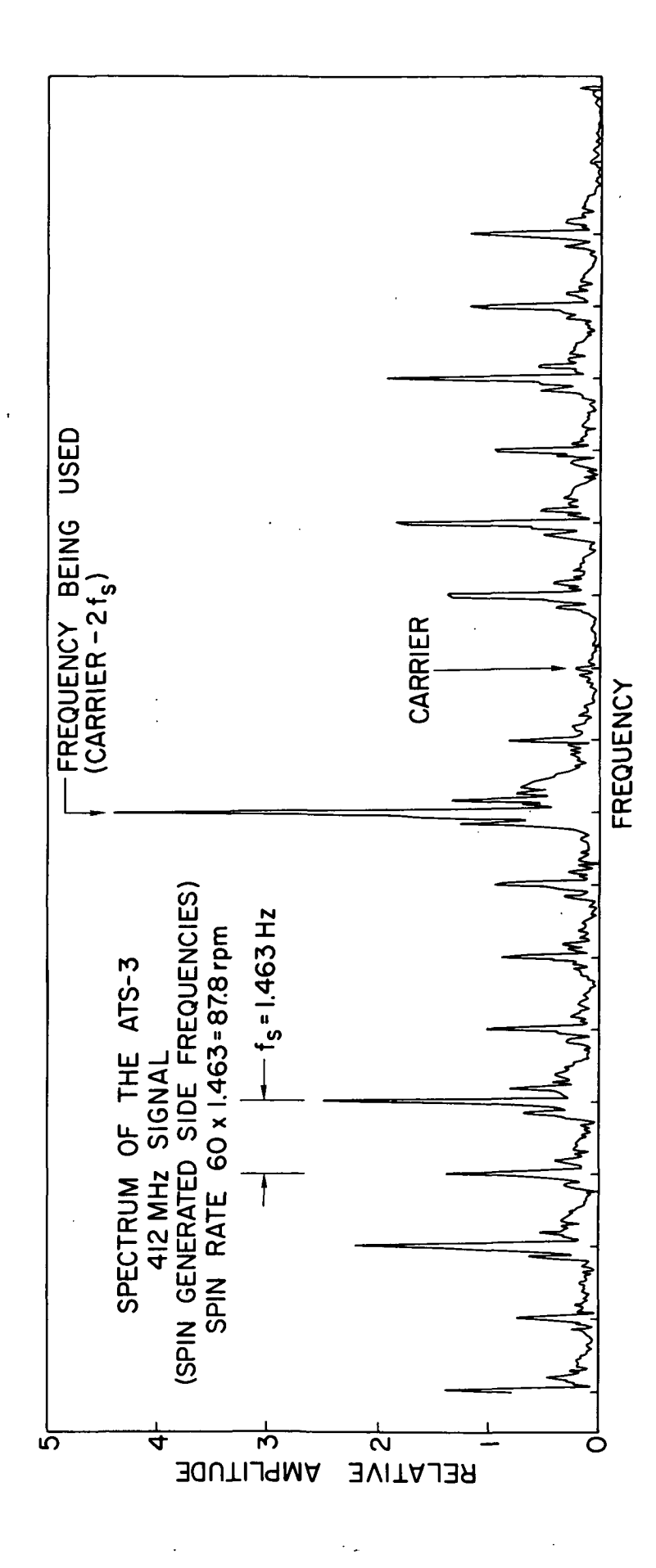
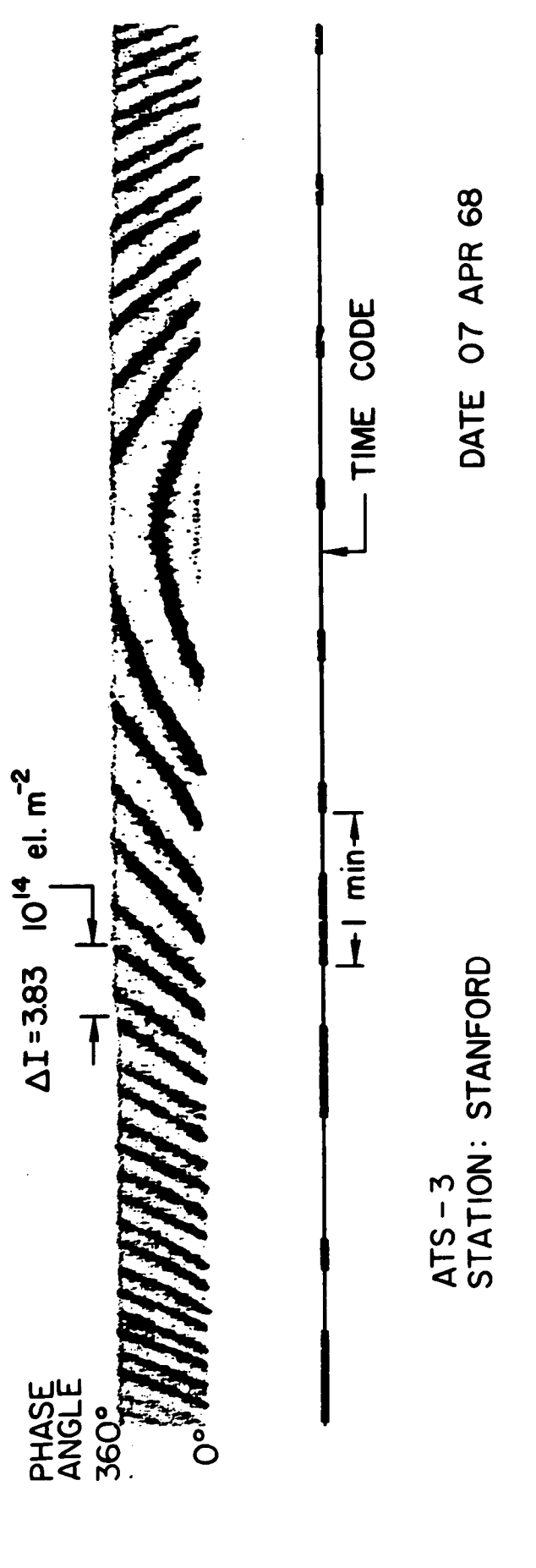


Fig. 1. ACTUAL SPECTRUM OF THE UHF SIGNAL RADIATED BY ATS-3.



this figure, one can see the ionization increase go through a maximum, Fig. 2. RETOUCHED PHOTOGRAPH OF THE DIFFERENTIAL DOPPLER FRINGES. In and then start to decline.

$$f_b = 3f_{VHF(R)} - f_{UHF(R)} = 2f_S + \frac{8}{3}f_I$$

The desired frequency,  $f_{T}$  is then

$$f_I = \frac{3}{8}(f_b - 2f_S)$$
 (14)

The subtraction of  $2f_S$  from the beat note  $f_b$  is done automatically in the receiver. To accomplish this, the UHF signal is demodulated and from the resulting low frequency audio tone, the component of frequency  $2f_S$  (which happens to be about 3 Hz) is extracted by means of filters. The beat note  $f_b$  and the component of frequency  $2f_S$ , are then multiplied by 4 and the difference is taken in a phase comparator. The output of the phase comparator is fed into a counter which counts the number of cycles of the signal. The accumulated count is, at regular intervals, read into a digital magnetic tape.

The relationship between the ionospheric Doppler shift f and the rate of change of slant columnar electron content is given by Equation (11)

$$f_{I} = QI$$
 (11)

where

$$Q = \frac{40.30}{cf_{VHF}} = \frac{1.344 \times 10^{-7}}{f_{VHF}} \text{ (MKS)}$$

and  $\tilde{I}$  is the time rate of change of the slant columnar electron content, I.

Between times t and t, the cycle count of f will be incremented by

count increment 
$$\int_{t_0}^{t} = \frac{32}{3} \int_{t_0}^{t} f_I dt = \frac{32}{3} Q (I - I_0)$$

where I is the (unknown) value of the slant content at to.

The slant columnar electron content increment is thus:

$$I - I_0 = \frac{3}{32 Q} \left( \text{count increment} \begin{bmatrix} t \\ t_0 \end{bmatrix} \right)$$
 (15)

The resolution is one count, resulting in a resolution of  $(3/32 \text{ Q}) \approx 9.6 \times 10^{13} \text{ el.m}^{-2}$  in the content measurement. This resolution could be increased by using a multiplying factor larger than four preceding the phase comparator.

To obtain a real time analog representation of the differential Doppler frequency,  $f_{T}$ , a technique is used involving the recording of the differential Doppler phase meter output which consists of a sawtooth wave with a frequency f,. Due to irregularities in the radiation pattern of the satellite, two small bumps appear on the ramp of the sawtooth wave. These bumps are, of course, synchronized with  $f_{\rm S}$  and thus will slip up or down the ramp by virtue of the fact that the sawtooth frequency, f, differs slightly from  $2f_S$ . If the recorder is run at a very low speed so that, as consecutive cycles of the sawtooth signal merge into each other, the bumps coalesce into figures that seem to move up or down along the graph, as in Figure 2. In this figure, one can see the ionization increase, go through a maximum, and then start to decline. Every other fringe in the figure is caused by the same one of the two bumps mentioned above. Thus the time interval between the start (or end) of two alternate fringes is the time that it took for the slant electron content to change by  $3.83 \times 10^{14} \text{ el.m}^{-2}$ .

## C. Determination of the absolute value of total columnar electron content

In this section it will be shown how the Faraday rotation angle,  $\Omega$ , can be combined with the columnar electron content increment,  $\Delta I = (I-I_0)$ , to yield a value of the parameter G provided uninterrupted measurements are available over a reasonably long period. Once a value of the parameter G, which relates Faraday rotation angle to total columnar electron content, is known at a time  $t_0$ , the value of the total electron content at that same instant of time is completely determined. The value of the total electron content at a time  $t_0$  is the constant of integration needed to convert differential Doppler frequency data into absolute values of total electron content.

In Chapter I, Section A it was shown that the Faraday rotation angle is related to the ionization along the ray path by

$$\Omega = \frac{Q_F}{f^2} \int_0^S nB_L \cdot ds$$
 (6)

where  $\Omega$  is measured in radians,  $Q_F$  is a constant with a numerical value of 2.36 x  $10^4$  in MKS units, f is the wave frequency in Hz, n is the concentration of electrons in m<sup>-3</sup>,  $B_L$  is the longitudinal component of the geomagnetic flux density in Wb m<sup>-2</sup>, and ds is an element of length along the ray path, in m.

A 'mean longitudinal geomagnetic flux density',  $\langle {\rm B}_{L} \rangle$  ,was defined such that Equation (6) can be written as

$$\Omega = \frac{Q_F}{f^2} \langle B_L \rangle \quad I = G \quad I \tag{9}$$

from which  $G = \frac{\Omega}{I}$  or, equivalently, at time  $t_0$ 

$$G_{o} = G(t_{o}) = \lim_{t \to 0} \left( \frac{\Omega(t_{o}) - \Omega}{I(t_{o}) - I} \right)$$
 (16)

where I is the total electron content of a reference electron concentration profile and  $\Omega$  is the Faraday rotation angle associated with the reference profile. In order that Equation (16) be meaningful it is necessary that I and  $\Omega$  go to zero simultaneously. The above condition is always satisfied for the QL propagation approximation. Under QL conditions the angle between the wave normal and the local geomagnetic field,  $\theta$ , is always in the same trigonometric quadrant so that  $\cos\theta$  does not change sign along the path of propagation. The longitudinal component of the geomagnetic field,  $B_L$ , does not change sign over the path of integration in Equation (6) and because electron concentration is always positive, I=0 implies  $\Omega$  = 0 and vice-versa.

The technique used to determine the parameter G is based on Equation (16), although the limit situation I = 0 is not observed in practice. Even during the night when the main generating source of the ionosphere, the solar EUV radiation, is absent, a residual ionization is always present. Except for very disturbed days, however, the residual nighttime ionization is small compared with day time electron concentration at the same levels in the ionosphere. Such large diurnal variation in the degree of ionization found in the ionosphere in most of the days, provided, therefore, a great deal of information which can help to determine the parameter G.

The quantities  $\Delta\Omega=(\Omega(t_0)-\Omega)$  and  $\Delta I=(I(t_0)-I)$  are experimentally determined from the Faraday rotation angle and the phase-path difference measurements, respectively. Values of the ratio  $\Delta\Omega/\Delta I$  can be computed

for decreasing values of I and  $\Omega$ . This is accomplished by selecting a time of the day,  $t_0$ , which is coincident or close to the time of maximum Faraday rotation angle, so that values of  $I(t_0)$  and  $\Omega(t_0)$  are very large compared to the corresponding nighttime values. Then by taking as reference values the smaller values of electron content and Faraday rotation angle at other times of the day the quantities  $\Delta I$  and  $\Delta \Omega$  can be determined and a collection of values of the ratio  $\Delta \Omega/\Delta I$  can be obtained. Plots of the ratio  $\Delta \Omega/\Delta I$  versus the variable  $\Omega$  are illustrated in Figure 3. It can be seen that for small values of  $\Omega$  the ratio  $\Delta \Omega/\Delta I$ , in general, converges in a rather well behaved way as  $\Omega$  decreases to its minimum observed value. The value of the ratio  $\Delta \Omega/\Delta I$  for  $\Omega=0$ , therefore, can be extrapolated from plots like the ones shown in Figure 3. Such value is by definition the value of the parameter G relative to time  $t_0$ .

The quantities  $\Delta\Omega$  and  $\Delta I$  are known very accurately and because the mean values of the ratio  $\Delta\Omega/\Delta I$  vary slowly for small  $\Omega$ , the estimated  $\pm$  7 degrees error in our determination of the Faraday angle has a negligible effect on the accuracy of the estimated value of  $\mathbf{G}_{0}$ . It is clear from Figure 3 that the closer the minimum values of the Faraday rotation angle come to zero, the more accurate the extrapolated value of  $\mathbf{G}_{0}$ . A criterion for the choice of the reference values is then established where the set of  $\Omega$  and I to be used will be the one which contains data points corresponding to a period of time in which the Faraday angle is decreasing to its minimum observed value during the entire period of continuous measurements of both variables. In general, the minimum value of Faraday rotation angle is observed right before sunrise at ionospheric heights and, provided such minimum value is low enough compared to the

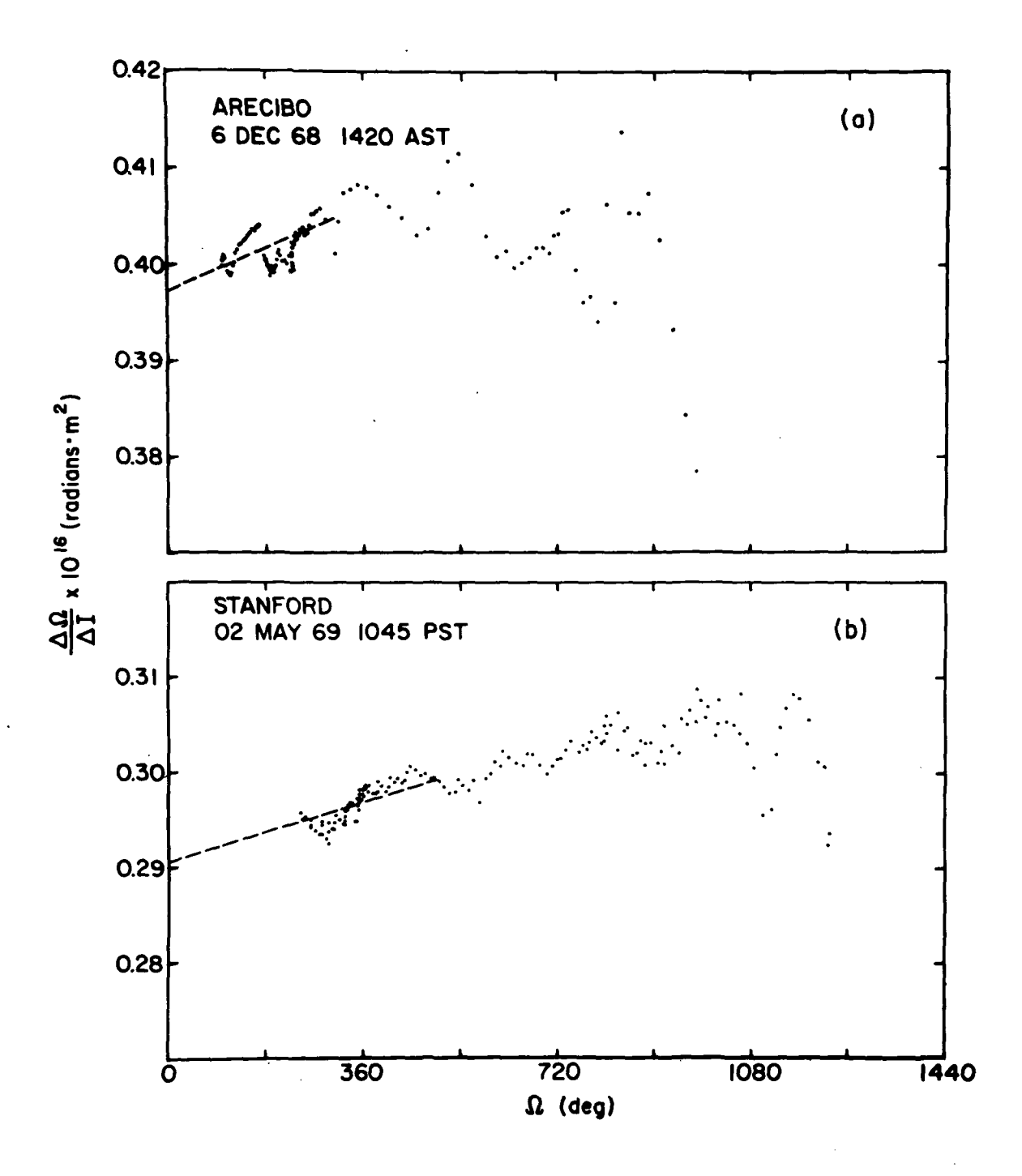


Fig. 3a,b. EXAMPLE OF PLOTS OF THE RATIO BETWEEN THE QUANTITIES  $\Delta\Omega=(\Omega(t)-\Omega)$  AND  $\Delta I=(I(t)-I)$  USED TO ESTIMATE VALUES OF THE PARAMETER G. It can be seen that the ratio for small values of  $\Omega$ , converges in a rather well behaved way as  $\Omega$  decreases to its minimum observed value. The dash line is the best estimate of  $\Delta\Omega/\Delta I$  convergence to its final value (the parameter G) for  $\Omega=0$ .

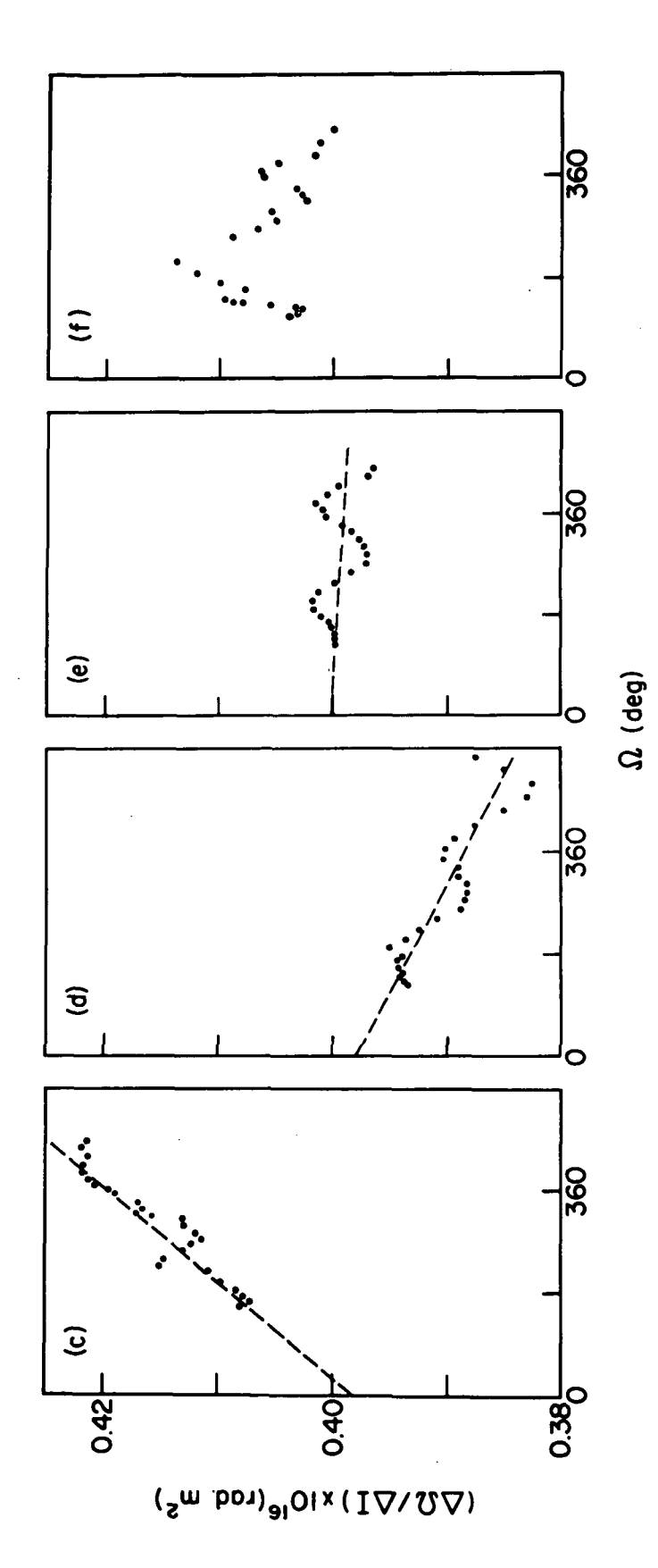


Fig. 3c, d, e, f. EXAMPLE OF PLOTS OF  $\Delta\Omega/\Delta I$  FOR ARECIBO; 06 DECEMBER 1968 AT 1420 AST. To form the quantities  $\Delta\Omega=(\Omega(t_0)-\Omega)$  and  $\Delta I=(I(t_0)-I)$  the values of I and  $\Omega$  were taken in the following intervals of time: c) from 1820 AST on 9 DEC 68 to 0600 AST on 10 DEC 68; d) from 0650 AST to 0815 AST on 8 DEC 68; e) from 0535 AST to 0810 AST on 9 DEC 68 and; f) from 0350 AST to 0800 AST on 7 DEC 68.

following daytime peak, very good determination of the parameter G can be made. Since the elapsed time between sunrise and daytime peak of the ionosphere is about 8 hours, this time turns out to be the minimum interval of continuous measurements of Faraday rotation angle and phase path difference data which can normally be useful for accurate estimates of the parameter G.

A value for I can be found from Equation (9):

$$I_o = I(t_o) = \frac{\Omega(t_o)}{G(t_o)}$$

Clearly the uncertainty in I depends on the accuracy in which both  $\Omega(t_0)$  and  $G(t_0)$  can be determined. The uncertainty which the parameter G was determined in all available data never exceeded  $\pm$  0.5%. The error in  $\Omega$  originates from two sources: the accuracy of the polarimeter equipment and the uncertainty in the determination of the initial polarization in which the wave is launched from the spacecraft. Because the error in  $\Omega(t_0)$  can be made negligible by improving the polarimeter and accurately measuring the initial polarization prior to the spacecraft launching, the accuracy in the value of I is solely limited by the uncertainty which  $G(t_0)$  can be determined, i.e., less than  $\pm$  0.5% of the daytime value of I. Such uncertainty corresponds to about  $\pm$  3 x  $10^{15}$  el.m<sup>-2</sup> which is at least one order magnitude lower than that of any other existing method of measuring columnar electron content.

The uncertainty in the values of I  $_{0}$  reported here, however, are of the order of  $\pm$  1% of the daytime value of I because the values of  $\Omega$  are affected by errors of about  $\pm$  7 degrees. Most of the error in  $\Omega$  comes from the determination of the initial polarization.

Once the absolute value of I at any particular moment has been determined, the value of I at any other time can be found from Equation (15). Provided there is no interruption in the data, the error in I is essentially the error in the determination of  $I_O$  because the resolution in the measurement of  $\Delta I$  is  $10^{14}$  el.m<sup>-2</sup>.

The knowledge of the columnar electron content, I, permits now the computation of G at any time during the period of continuous observations, through the use of Equation (9):

The analysis discussed above yields a description of the diurnal behavior of the total columnar electron content and of the parameter G.

To illustrate the method of determination of I, let us consider the plot shown in Figure 4. It represents the total electron content, I, vs. time as obtained at Arecibo. At this stage of the analysis the exact shape of the I vs. t curve is known from the phase-path difference experiment; what is missing is the integration constant, I, at any arbitrary time, to, i.e. the exact position of the curve on the ordinate scale. (The ordinate on Figure 4 was labeled 'a posteriori'.) The best value of I is being sought. It can be seen that during the interval of time between the daytime peak on 6 December and the sunrise in the next morning. the content decayed to its minimum value observed during the period of measurements. Although not shown in this figure, the Faraday rotation angle also decayed to its minimum observed value, so that we select the above mentioned interval of time for taking the reference values of  $\Omega$  and I. Time t corresponding to  $\Omega$  and I is the time of the content peak on the 6th, i.e. 1420 AST. The quantities  $\Delta I = (I(t_0) - I)$  and  $\Delta\Omega = (\Omega(t_0) - \Omega)$  were formed and the corresponding values of the ratio

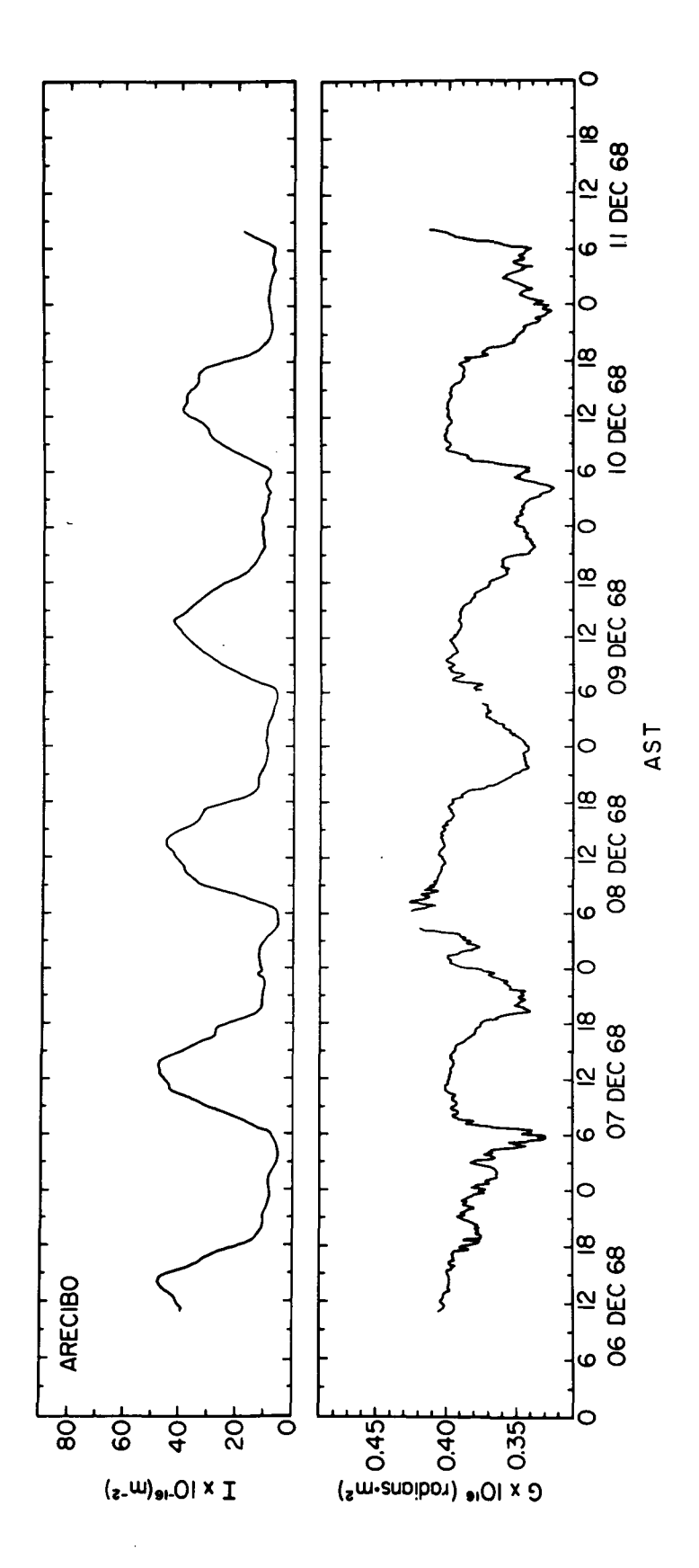


Fig. 4. DIURNAL VARIATION OF THE TOTAL SLANT ELECTRON CONTENT, I, AND OF THE PARAMETER G, FOR SEVERAL DAYS IN DECEMBER 1968. The observation was made at Arecibo using the geostationary satellite ATS-3 when it was drifting from -47.4° E to -50° E.

 $\Delta\Omega/\Delta I$  were plotted versus  $\Omega$  in Figure 3a. The value of 0.3970 x  $10^{-16}$ radians.m<sup>2</sup> for G at 1420 AST (Antilles Standard Time) on 6 December 1968, was obtained by extrapolation. The plots of  $\Delta\Omega/\Delta I$  labeled c.d.e. and f in Figure 3 were obtained from the Arecibo data of 6 December 1968 at 1420 AST, by selecting other intervals of time as reference values of  $\Omega$  and I. The behavior of  $\Delta\Omega/\Delta I$  for small values of  $\Omega$  in the first three plots is such that good extrapolations for the value of G can be made. The scatter in the extrapolated values of G; corresponding to plots a,c,d, and e, is less than ± 0.5%. Plot f corresponds to a case in which the convergence of  $\Delta\Omega/\Delta I$  is not well defined and no attempt to extrapolate a value for G was made in such cases. The value of the Faraday rotation angle at 1420 AST was (1082 ± 7) degrees thus the total columnar electron content at that instant of time obtained by using Equation (9) is  $(47.55 \pm 0.48) \times 10^{16}$  el.m<sup>-2</sup>. Now that a value of I has been found, the total columnar electron content, I, is determined via Equation (15). The parameter G is then determined for any time during the period of observations via Equation (9), and it is shown in Figure 4 together with I.

Figure 4 shows the diurnal behavior of G a quantity which tends to be large and constant during the day, falling off in the afternoon to the lower nighttime values and finally rising very fast at dawn to its daytime level. Fluctuations of as much as 7.5% in the daytime values of the parameter G were observed during that period. The minimum values of G, during the night, were 22% lower than its mean daytime level.

An alternative method for the determination of a value of G using the time derivatives of the quantities  $\Omega$  and I has been developed (Almeida

et al.[1970]).

Taking the time derivative of Equation (9):

$$\hat{\Omega} = GT + TG$$

and, since from Equation (9),  $I = \Omega/G$ 

$$\overset{\circ}{\text{IG}}^2 - \overset{\circ}{\Omega} G + \overset{\circ}{\Omega} G = 0 \tag{16}$$

Equation (16) is a differential equation in G in which the coefficients,  $\stackrel{\circ}{\Omega}, \stackrel{\circ}{\Omega}$  and I are all quantities derived from experimental observations.

It can be seen that, if, throughout the day, a time, to, can be found on the G is zero and  $\Omega$  and I are non zero, then, at that moment,

$$G_{o} \equiv G(t_{o}) = \frac{\mathring{\Omega}(t_{o})}{\mathring{I}(t_{o})}$$
 (17)

hence a value for I can be found from Equation (9) which becomes:

$$I_o = I(t_o) = \frac{\Omega(t_o)}{G(t_o)}$$

The values of  $\Omega$ ,  $\overset{\circ}{\Omega}$ , and  $\overset{\circ}{I}$  do not contain enough information to permit a mathematical determination of the time periods when  $\overset{\circ}{G}=0$ . This is equivalent to saying that it is impossible to extract initial conditions from a differential equation; initial conditions must come from independent considerations. In the present work it is necessary to examine the physical processes involved and select all time periods when it is most plausible to assume that there are no changes in G, and then support this selection by means of self consistency checks.

Constant G is implied by an ionization profile with unchanging shape and unvarying height. It is reasonable to expect that the shape and

height are best preserved near the middle of the day (or of some nights) when layer height and plasma temperature and composition are themselves unchanging.

A careful scrutiny of all available data is made in order to identify the time periods during which G is judged to be zero and the time rates of change of  $\Omega$  and I are not negligible. As many such periods as possible are selected. Each selected period yields an independent initial condition for the differential equation; if the assumptions made were perfectly correct and if the data contained no uncertainties, then these initial conditions would be redundant. In practice each initial condition leads to a slightly different solution and all reasonable solutions are considered together to determine the most probable one by means of a simple error minimizing technique described further on.

To illustrate the method of selecting a period when G=0, let us consider the plot of the total electron content, I vs. time obtained at Stanford, and shown in Figure 5. It can be seen that near noon on April 6 and 7 there are intervals of time when the content changes reasonably fast. Although not shown in this figure, the Faraday rotation angle also changes during this period, so that I and  $\Omega$  are non negligible. Assuming that G was unchanging during those periods in question, four independent values of G, indicated in Table 1, were obtained by using Equation (17).

Using these four independent values, the integration constant  $I_o$  was found by minimizing the quadratic error in the following manner: Let  $\Delta I_i = \int_t^{t_i} \overset{\circ}{I} \, dt$ . At time  $t_i$  the true columnar content will be  $I_o + \Delta I_i$ . Let  $I_o$  be the columnar content estimated for the time  $t_i$  by assuming  $\overset{\circ}{G} = 0$  at that time. The mean square error between the estimated and the

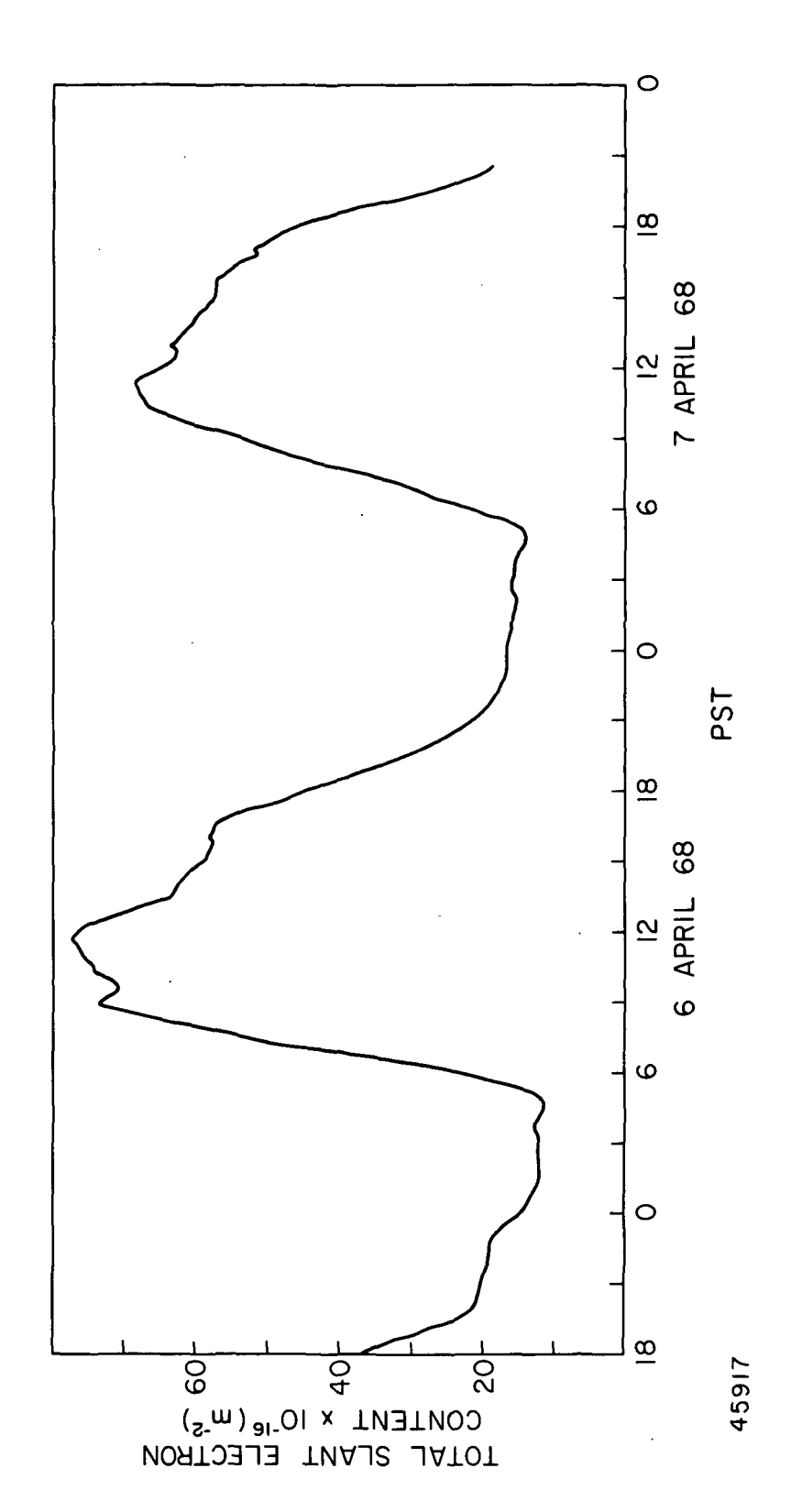


Fig. 5. DIURNAL VARIATION OF THE TOTAL ELECTRON CONTENT OF THE PLASMASPHERE. The observation was made from Stanford using the geostationary satellite ATS-3 when it was around -82° E.

true values is

$$\overline{e^2} = \frac{1}{N} \sum_{i=0}^{N} (i_{oi} - i_{o} - \Delta i_{i})^2$$

where N is the number of independent estimates of I made.

TABLE 1

DATE	TIME (PST)	$G_0 \times 10^{16}$ rad.m	$G \times 10^{16}$ rad.m <sup>2</sup>	Deviation of G o (percent)
6 Apr 68	12:15	0.3503	0.3522	-0.53
6 Apr 68	12:50	0.3523	0.3520	+0.08
6 Apr 68	13:12	0.3523	0.3503	+0.57
7 Apr 68	11:52	0.3509	0.3508	+0.02

Table 1. Comparison between the form factors, G calculated independently and the factor, G obtained from the least error analysis.

The value of I  $_{\rm O}$  which minimizes the quadratic error can be found by setting

$$\frac{d\varepsilon^2}{dI_0} = 0$$

This yields

$$I_{o} = \frac{1}{N} \sum_{i=1}^{N} (I_{oi} - \Delta I_{i})$$
 (18)

The knowledge of I  $_{\rm O}$  from Equation (18) permits the determination of I and G at any time. The values of G thus calculated are indicated in Table 1, together with the deviations from the individual determination of G  $_{\rm O}$ .

The apparent simplicity of the method is somewhat deceptive; it is based on the premise that a moment of the day when  $\mathring{G}=0$  and  $\mathring{\Omega}$  and  $\mathring{I}$  are non-negligible can be found. Since G does not increase or decrease indefinitely, moments when  $\mathring{G}=0$  do exist. Such moments, in general, coincide with the middle of the night when  $\Omega$  and I are near constant and with the middle of the day when  $\Omega$  and I are slowly evolving through the maximum of the diurnal variation. This behavior turns out to be unfavorable when time derivatives of the quantities  $\Omega$  and I are to be taken. Furthermore, the differentiation operation on the variables in question enhances the noise level causing a deterioration on the accuracy which  $\mathring{\Omega}$  and  $\mathring{I}$  can be estimated. Nevertheless this alternative method could be useful in cases in which the technique of extrapolation of the ratio  $\Delta\Omega/\Delta I$  becomes difficult. Such cases may exist when the minimum observed value of Faraday rotation angle is not low enough to assure a reliable extrapolation of the ratio  $\Delta\Omega/\Delta I$  for  $\Omega=0$ .

A comparison between the values of G derived by the two methods described here, for the 6-7 April 1968 data, was made. The technique of extrapolation of the ratio  $\Delta\Omega/\Delta I$  yields daytime values of G 2% higher than the corresponding values of G determined by the second method. Because this is one case where very reliable extrapolation of the ratio  $\Delta\Omega/\Delta I$  could be done, the above mentioned difficulties with the alternative method can explain the discrepancy between the values of G.

# Page Intentionally Left Blank

# CHAPTER III

TECHNIQUE OF PROTONOSPHERIC ELECTRON CONTENT DETERMINATION USING GEOSTATIONARY SATELLITES:

Owing to the fact that the Faraday rotation angle is related to the product of electron concentration and the longitudinal component of the geomagnetic field, signals traversing the plasmasphere are relatively unaffected by the ionization at high altitudes where the geomagnetic field is quite weak. The phase-path difference, on the other hand, is a quantity equally sensitive to ionization at any altitude. The observed changes in phase-path length are, thus, a measurement of changes in the total ionization encountered along the path of propagation. This suggests the possibility of inferring information on electron content of the upper regions of the plasmasphere by combining Faraday rotation angle and phase-path difference data.

Howard et al.[1964a], Howard et al.[1964b], Howard[1967] and Yoh [1968], using lunar radar echoes and da Rosa[1965], da Rosa and Almeida [1968], using satellite transmissions, tried to determine the so called 'relative protonospheric electron content',  $\Delta I_p$ . The scheme used was to subtract from the columnar electron content increment,  $\Delta I_p$ , derived from the phase-path difference data, the 'Faraday electron content',  $I_p$ , a quantity proportional to the Faraday rotation angle data.

$$\Delta I_{p} = \Delta I - I_{F} = \Delta I - \frac{\Omega}{G_{I}}$$
 (19)

where  $\mathbf{G}_{\mathbf{I}}$  is the value of the parameter G corresponding to the value of  $\mathbf{B}_{\mathbf{r}}$  computed at a height of approximately 400 km.

It was assumed that the parameter  $G_{I}$  calculated in this way would convert Faraday rotation angle data into electron content of the 'ionosphere', the region below 1000 km.

The parameter  $G_I$  depends on the geometry of the distribution of  $B_L$  and on the shape and height of the electron concentration profile along the ray path (Yeh and Gonzales[1960], Almeida et al.[1970], and Smith [1970]). Based on the knowledge that the shape and height of the electron concentration profile, in the ionosphere, changes during the day, some of the authors mentioned in the beginning of the section, tried to improve their determination of  $\Delta I_p$ , correcting the values of  $G_I$  for changes in the height of the peak of electron concentration.

The above procedure involves a fallacy in that it implies that Faraday rotation abruptly ceases above a determined level. Consequently, the mentioned procedure leads to an improper interpretation of  $\Delta I_{p}$ .

The analysis which follows below will show that the quantity  $\Delta I_p$  defined by Equation (19) is not a measure of the relative electron content above a determined level but may nevertheless yield useful information on the electron content of the upper region under certain geometries of observation.

# A. Analysis

It was shown in Chapter 2, Section C, that by combining Faraday rotation angle and phase-path difference data measured using VHF and UHF transmissions from geostationary satellites, it is possible to determine very accurately the columnar electron content. It is convenient then to rewrite Equation (19)

$$I_{w} = I - \frac{\Omega}{G_{I}}$$
 (19a)

SEL-72-019

where I is the columnar electron content derived from phase-path difference data.

With the aid of Equations (6) and (8), Equation (19a) can be further rewritten as

$$I_{w} = \int_{0}^{S} n (1 - \frac{B_{L}}{B_{LI}}) ds = \int_{0}^{S} n W ds$$
 (19b)

where  $\textbf{B}_{L\,I}$  is the value of  $\textbf{B}_{L}$  corresponding to  $\textbf{G}_{I}$  and n is the local electron concentration.

The quantity I  $_{\rm W}$  defined by Equation (19b) is the electron content weighted by the function W  $\equiv$  (1 - B  $_{\rm L}/{\rm B}_{\rm LI}$ ) along the observer-to-spacecraft path.

The conditions which must be satisfied for  $I_W$  to be the electron content of the region extending upwards from a determined level, corresponding to the length  $S_i$  along the path of integration, to the spacecraft are given by

$$\int_{0}^{S} n (1 - B_{L}/B_{LI}) ds = 0$$
 (20)

and

$$\int_{S_{i}}^{S} n (1 - B_{L}/B_{LI}) ds = \int_{S_{i}}^{S} n ds, or$$

$$B_{L}/B_{LI} = 0, \text{ for } s > S_{i}$$
(21)

Because the ionospheric physicist is interested in having information on the protonosphere - the region in which the Hydrogen ions,  $\mathrm{H}^+$ , are the dominant species - the level being considered here is near the  $\mathrm{H}^+$  transi-

tion height, i.e., the level where the concentration of H<sup>+</sup> ions is 50% of the total ion concentration, and which lies approximately in the altitude range from 800 to 2000 km and is well above the F region electron concentration peak.

For a given geometry of observation, the longitudinal component of the geomagnetic field,  $B_L$ , is determined and a value of  $B_{LI}$  must be found such that Equations (20) and (21) are reasonably approximated for any profile n(s) which might exist. In the case of midlatitude stations it is in general possible to find a value  $B_{LI}$  which satisfies Equation (20) for a given electron concentration profile. This value of  $B_{LI}$  is of the order of the values of  $B_L$  in the region of consideration in Equation (20) and because  $B_L$  does not decay very fast with height, the condition imposed by Equation (21) is far from being satisfied. The problem of finding a value for  $B_{LI}$  which satisfies this latter equation becomes even more complicated because n(s) profiles vary with time and are not known in general.

For  $I_w$  to be a measure of the electron content of the protonosphere, the ideal geometry would be one in which  $B_L$  is constant in the ionosphere and then falls off very fast above the transition level. Under such circumstances it would be possible to find a value  $B_{LI}$  such that W is zero in the ionospheric region and becomes approximately equal to unity in the protonosphere; the conditions expressed by Equations (20) and (21) would then be satisfied for any profile n(s).

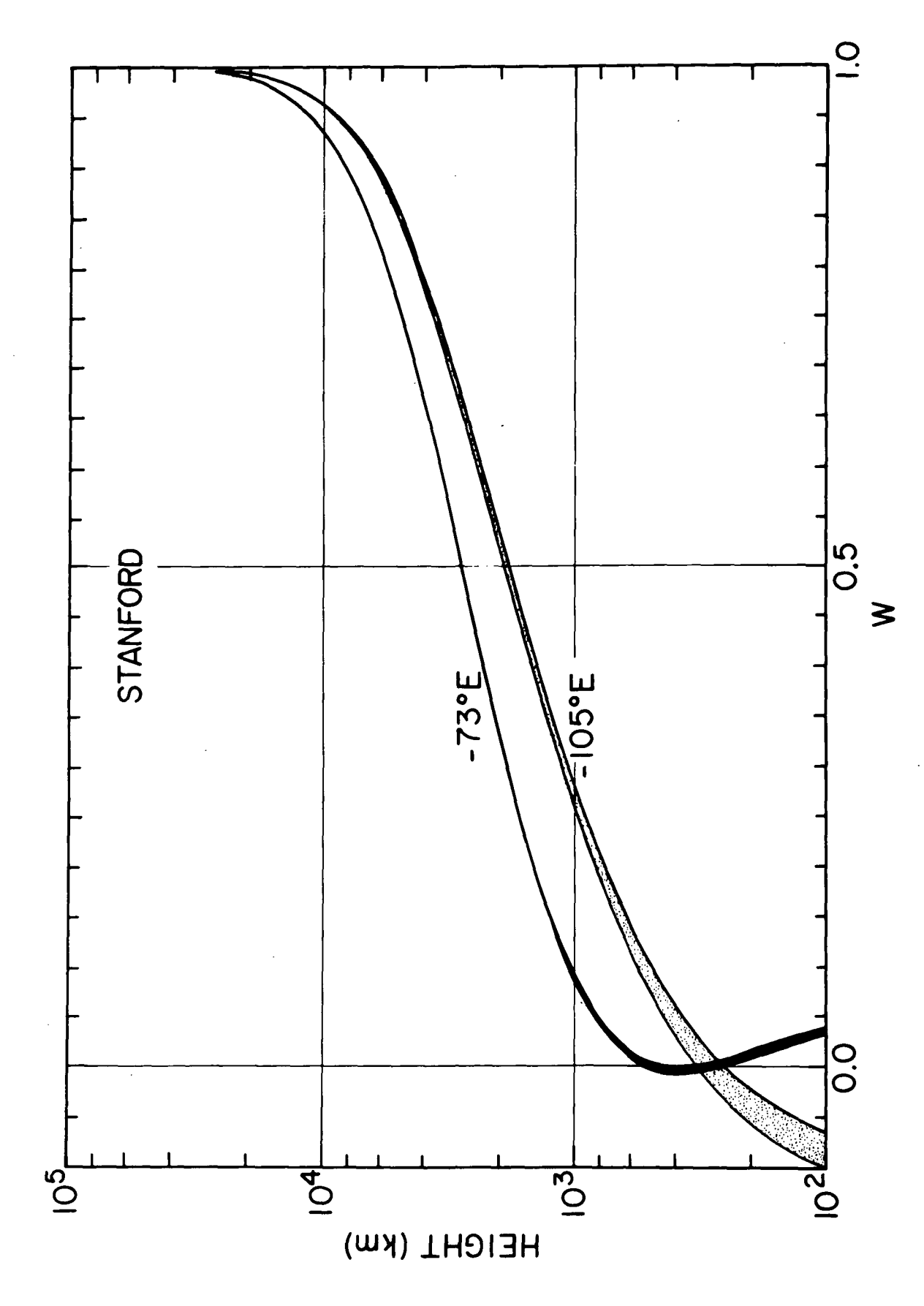
Unfortunately the <u>ideal</u> geometry mentioned above cannot be found because of the smooth way the geomagnetic field varies with height. In practice, however, geometries which approximate the ideal one quite

satisfactorily can be found, at least, for an observer at geomagnetic midlatitudes. An analysis of the geometries which can occur for observers at Stanford and Arecibo will follow.

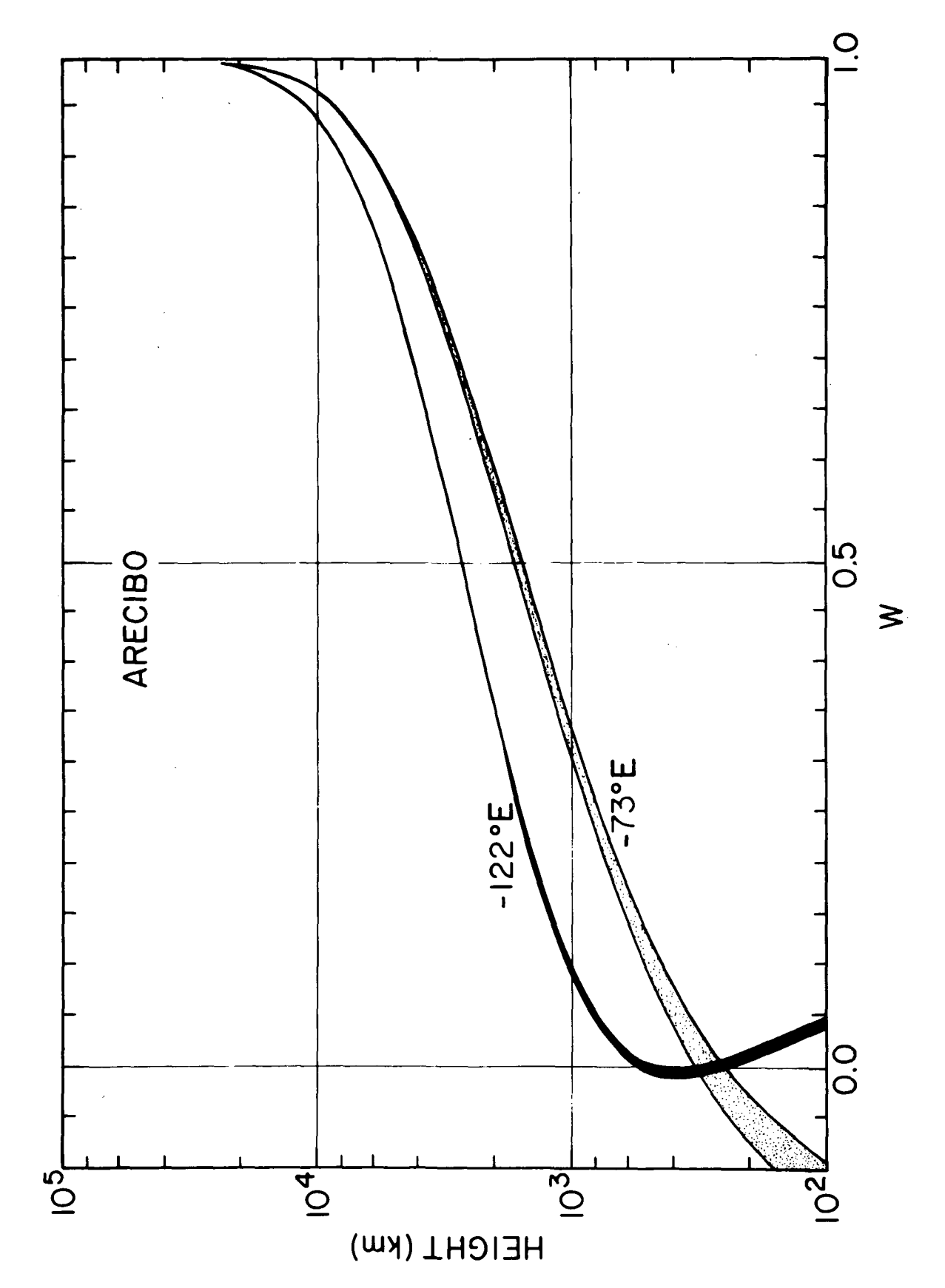
The variation of  $B_L$  with height along the observer-to-satellite path can be such that: a)  $B_L$  is a decreasing function of height all the way along the path; b) in the region extending from observer to, say 600 km,  $B_L$  is nearly constant and then starts decreasing very slowly with height. In this second case it is possible to find a value  $B_{LI}$  such that Equation (20) is reasonably well satisfied for any n(s) profile for levels below some 800 km. Clearly, it is not possible to find such value  $B_{LI}$  for case (a).

Values of the function W were computed along the observer-to-satellite path for Stanford (-122.16°E, 37.4°N) and for Arecibo (-66.85°E, 18.4°N). Several possible geometries of observation covering the range of longitudes where a geostationary satellite would be visible from each station, were considered. Very accurate values of geomagnetic field, estimated from the recent POGO(8/69) coefficients (see Cain and Sweeney[1970]), were used in the calculations of W. Given the positions of both the station and the satellite, a family of curves W vs. height can be generated corresponding each one to a different value of B<sub>LI</sub>. The values of B<sub>LI</sub> chosen to generate one family of curves correspond to values of B<sub>L</sub> computed at points on the observer-to-satellite path with height ranging from 250 km to 350 km approximately. The plots of W, shown in Figures 6 and 7, illustrate the behavior of such families of curves, for Stanford and Arecibo stations respectively.

When the observer is at Stanford and the satellite parked at -105° E,



families of W are shown corresponding to geostationary satellites positioned at -73° E Fig. 6. PLOTS OF THE WEIGHT FUNCTION W VERSUS HEIGHT FOR AN OBSERVER AT STANFORD. Two and -105° E.



families of W are shown corresponding to geostationary satellites positioned at -73° E and -122° E. Fig. 7. PLOTS OF THE WEIGHT FUNCTION W VERSUS HEIGHT FOR AN OBSERVER AT ARECIBO. Two

the variation of  $B_L$  conforms to case (a), above. It can be seen in Figure 6 that in this case the various curves of W are increasing functions of height. The curves of W merge into one another at very high altitudes such that W has the value of approximately 0.5 around 1800 km and is greater than 0.9 above 8000 km.

For the same observer at Stanford, and the satellite now parked at -73° E the resultant geometry is of the type (b). The family of curves W stays very close to zero in the range from 100 to 600 km (see Figure 6) and then starts to increase, merging into each other at heights lower than in the previous case. The weight function W has the value 0.5 around 2800 km and is greater than 0.9 above 8000 km.

Very similar situations can be found for an observer at Arecibo. As can be seen from Figure 7, geometries corresponding to types (a) and (b) are found for satellite positions -73°E and -122°E, respectively.

The plots of W in Figures 6 and 7 indicate that there are some geometries in which the ionospheric electron content contribution to  $\rm I_w$  can be pretty much eliminated by a convenient choice of the parameter  $\rm B_{LI}$  which causes the resultant W to be reasonably constant and close to zero at ionospheric heights. Those are the cases for Stanford with the satellite at -73° E, and Arecibo with the satellite at -122° E, cases which are going to be denoted from now on as Stanford/73 and Arecibo/122, respectively. The other examples shown in the figures, (Stanford/105 and Arecibo/73) are not favorable in the sense of eliminating the contribution of the ionospheric content to  $\rm I_w$  for the reasons already discussed in the beginning of this section.

Values of  $I_{w\ell} = \int_0^{800} n \text{ W sec } \chi \text{ dh were computed for several different}$ 

geometries using backscatter electron concentration profiles representative of different hours of the day (courtesy of D.H. Smith). For each station-satellite position, several different values of  $B_{LI}$  were used in the computations of  $I_{w\ell}$ . Plots of  $I_{w\ell}$  versus time, for a period of 24 hours, in Figure 8, show that for the geometry Stanford/73 a value  $B_{LIo}$  can be found such that the corresponding values of  $I_{w\ell}$  are very small, never exceeding the limits  $\pm 0.1 \times 10^{16} {\rm el.m}^{-2}$ , and do not correlate with the values of  $I_{\ell} \equiv \int_0^{800} n \sec \chi \, dh$ , also shown in the same figure. The values of  $I_{\ell}$  under consideration in the figure are comparable to observed values of electron content:  $60 \times 10^{16} {\rm el.m}^{-2}$  during the day, and  $10 \times 10^{16} {\rm el.m}^{-2}$  for nighttime. Even in the extreme case of  $I_{\ell}$  reaching values double of those given above, the corresponding values of  $I_{w\ell}$ , for the same electron concentration profiles used for test, will not exceed  $\pm 0.2 \times 10^{16} {\rm el.m}^{-2}$ .

For a value of the parameter  $B_{LI}$  1% higher than the optimum value  $B_{LIo}$ , the corresponding values of  $I_{w\ell}$  for the daytime profiles increase substantially so that they strongly correlate with the corresponding values of  $I_{\ell}$ , as it is clear from Figure 8. An inverse correlation between  $I_{w\ell}$  and  $I_{\ell}$  is obtained when the value of the parameter  $B_{LI}$  used to compute  $I_{w\ell}$  is lower than  $B_{LIo}$ , a case which is also shown in Figure 8. This shows the great sensitivity of the values of  $I_{w\ell}$  to relatively small variations in  $B_{II}$ .

For geometries of the type (a), such as Arecibo/73, plots of  $I_{w\ell}$  obtained using the same backscatter electron concentration profiles of the previous case, shown in Figure 9, indicate that variation of  $I_{w\ell}$  greater than 0.7 x  $10^{16}$ el.m<sup>-2</sup> occurs even for the optimum value of  $B_{LI}$ 

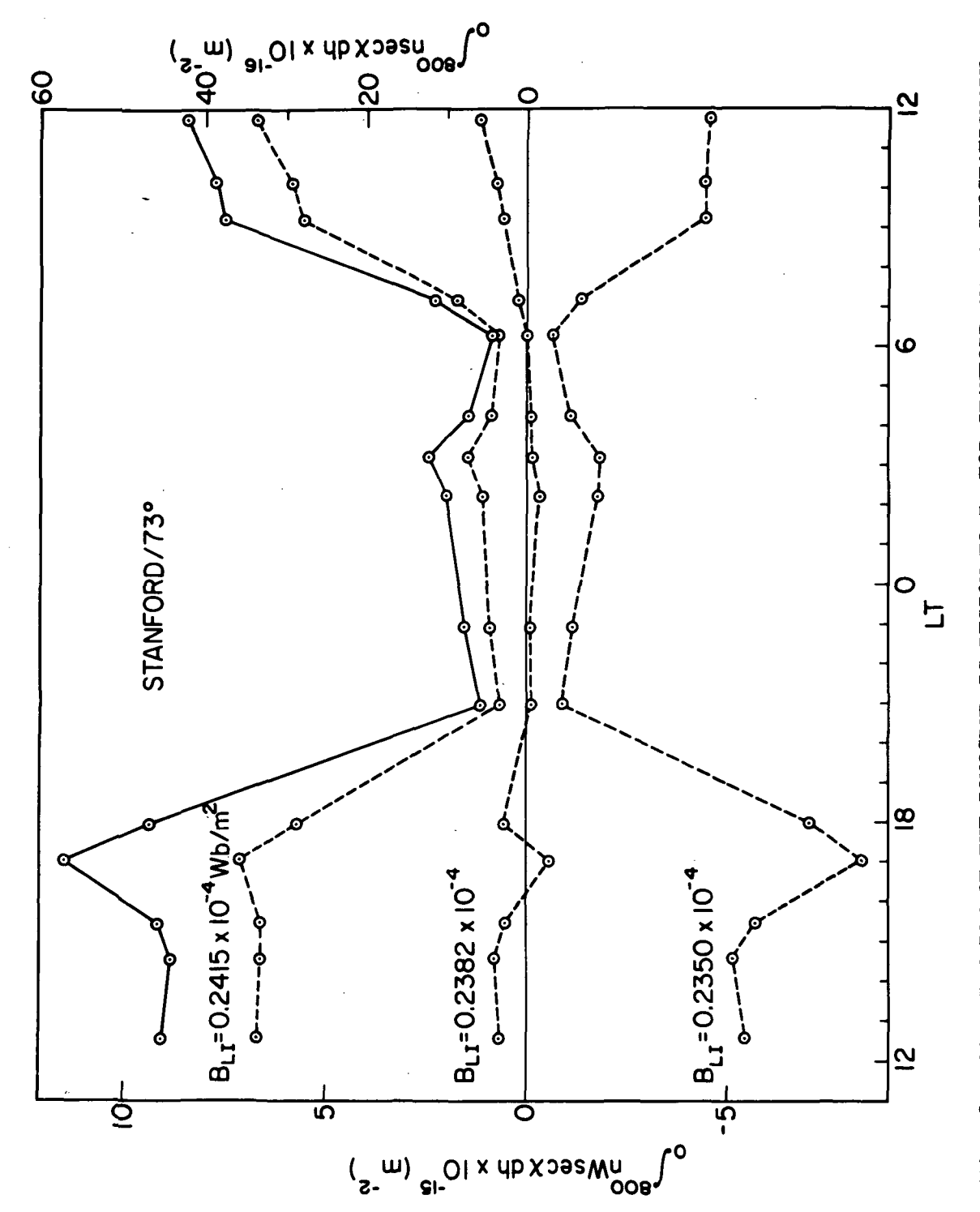
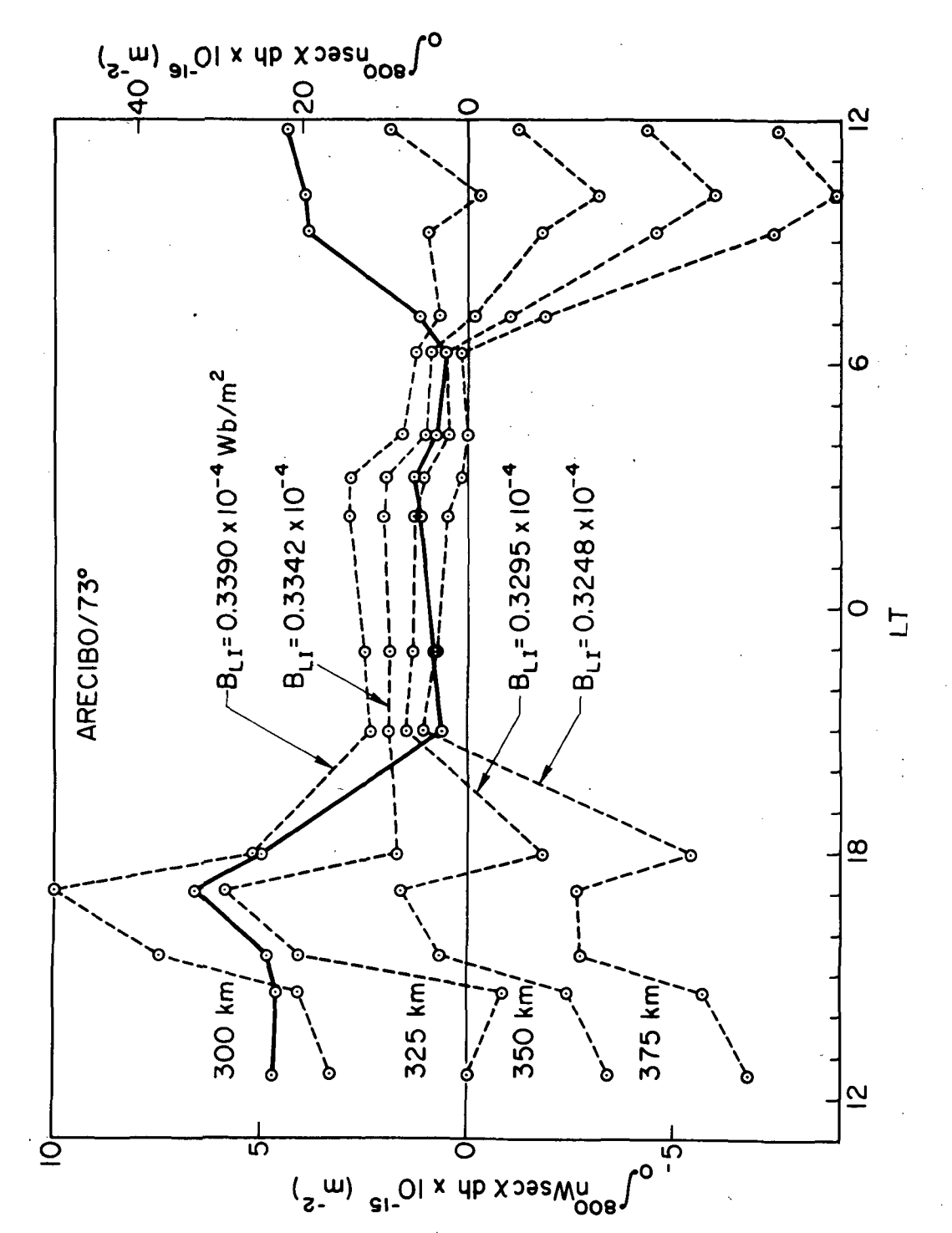


Fig. 8. CONTRIBUTION OF THE IONOSPHERIC REGION TO I FOR STANFORD AND A GEOSTATIONARY SATELLITE AT -73° E. The curves of I for three different values of B (circles connected by dash line) were computed using representative ionization profiles covering a period of 24 hours. Values of the electron content, I  $_{\ell}$ , associated with each profile are shown by circles connected by the solid trace.



.6. 9. CONTRIBUTION OF THE IONOSPHERIC REGION TO I FOR ARECIBO AND A GEOSTATIONARY SATELLITE AT -73° E. The curves of I for three different values of B (circles connected by dash line) were computed using representative ionization profiles covering a period of 24 hours. Values of the electron content, I, associated with each profile are shown by circles connected by the solid trace. Fig. 9.

which correspond to a height of 350 km. In the extreme case of  $I_{\ell}$  reaching values double of the ones used in the computations the corresponding variation of  $I_{w\ell}$  can be 1.5 x  $10^{16}$ el.m<sup>-2</sup> a value which is about the same order of the protonospheric content.

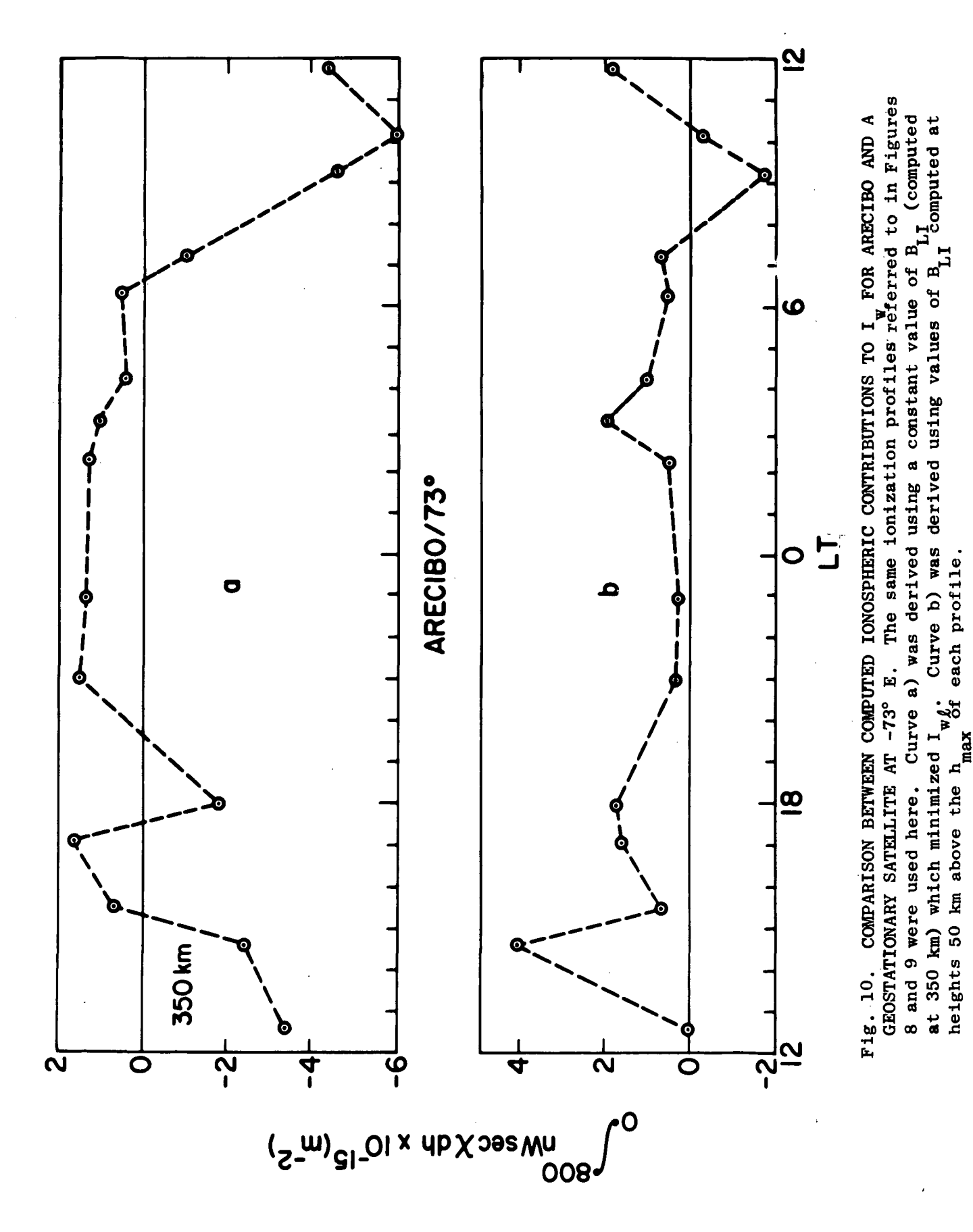
It was already discussed in the beginning of this Section that it is possible to find a value  $B_{LI}$  which satisfies Equation (20),  $I_{w\ell} = 0$ , for a given electron concentration profile. It is clear, therefore, that a reasonable knowledge of the shape and of  $h_{max}$ , the height of the electron concentration peak, of the actual profiles, is necessary in order to estimate values of  $B_{LI}$  which reasonably minimize the variations of  $I_{w\ell}$ .

Information on the height h can be obtained from ionograms but they yield electron concentration information of only the bottom side of the ionosphere. The situation is improved by the use of Thomson Scatter records which can cover the altitude range of the ionosphere, although such records are costly and can be obtained only in a few locations.

A procedure often used in the past for minimizing the variation in  $I_{\text{w$\ell}} \text{ is to adopt values of B}_{\text{LI}} \text{ computed at heights 50 km above the observed } h_{\text{max}}.$ 

Figure 10 compares plots of  $I_{w\ell}$  calculated by the above procedure with values of  $I_{w\ell}$  obtained by using a constant value of  $B_{LI}$  computed at a fixed height of 350 km. The 'corrective' procedure does not greatly reduce the values of  $I_{w\ell}$  which are shown in the figure to have variation of the same order as those resulting from the use of a fixed height.

From the comparison between the two geometries, Stanford/73 and Arecibo/73, discussed above, it is evident that the elimination of the ionospheric electron content from the total observed  $I_{\overline{w}}$  is better accom-



Curve b) was derived using values of B LI

heights 50 km above the h max

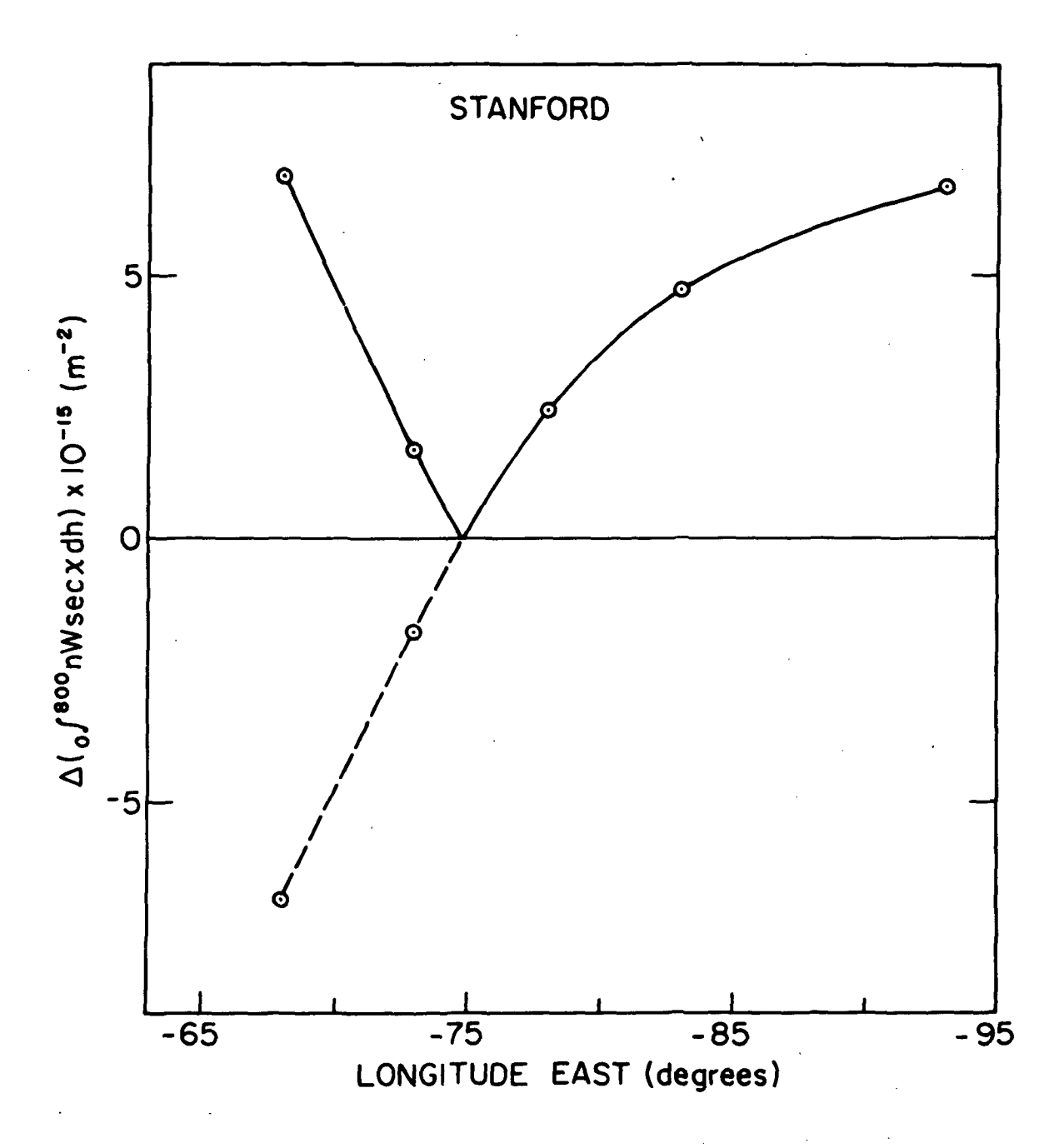


Fig. 11. PLOT OF THE MAXIMUM COMPUTED FLUCTUATION OF IONOSPHERIC CONTRIBUTION TO I , FOR STANFORD, VERSUS SATELLITE LONGITUDE.

plished for geometries of the type (b). For geometries of the type (a), such as Arecibo/73, the knowledge of the ionization profile covering the heights of the ionosphere would be desirable.

One question arises of how critical the satellite position is, for the favorable geometries of type (b), when the elimination of the ionospheric electron content is being sought. Again, taking the backscatter profiles for test, and assuming the observer to be at Stanford, values of  $I_{w\ell}$  for several satellite positions around-73°E were computed, using in each case, the optimum value of  $B_{LI}$ . The maximum computed variation of  $I_{w\ell}$  is plotted vs. satellite longitude in Figure 11. Interpolation between the computed values indicate that the most favorable satellite longitude is near-75°E. Displacements of  $\pm 4^\circ$  in longitude around-75°E correspond to maximum variations in  $I_{w\ell}$  of 0.3 x  $10^{16}$ el.m<sup>-2</sup> a value about one order of magnitude lower than the protonospheric content in normal days.

A very fortunate coincidence is the fact that most of the long runs of uninterrupted data collected at Stanford (a total of 320 hours) were obtained when the geostationary satellite ATS-3 was at -73° $\pm$ 0.5°E. It is, therefore, of interest to interpret the meaning of the measured I in terms of columnar electron content of the upper regions of the plasmasphere for that geometry of observation.

The measured  $I_w$  can be considered as the sum of three partial contributions, the ionospheric part,  $I_{w\ell}$ , the part corresponding to the region ranging from 800 km to 10,000 km,  $I_{wi}$ , and the contribution of the region extending from 10,000 km to the satellite height,  $I_{wi}$ .

For the Stanford/73 geometry, adopting the optimum value of the parameter  $B_{LI}$ ,  $I_{w\ell}$  is practically zero. The value of W (see Figure 6) is very

close to unity (W > 0.95) at heights above 10,000 km, therefore,  $I_{wu}$  approximates the electron content of the region extending from 10,000 km to the satellite height (35,600 km) with a resolution better than 5%. It is not clear, however, how much of the ionization which lies in the range from 800 km to 10,000 km contributes to  $I_{w}$  because it depends on how the product n.W, (electron concentration times the weight function W) varies with height along the observer-to-satellite path.

Estimates of the dependence of  $I_w$  on the electron content of the upper region were made based on the extrapolation of the backscatter profiles, above 800 km, by using a diffusive-equilibrium model of the field-line distribution of ionization (Angerami[1966]). The parameters of the model are ion and electron temperatures, which are assumed to be equal to one another and independent of height, and the relative concentrations of  $0^+$  and  $H^+$  at the 800 km reference level. For each of the backscatter profiles, several extrapolations were made varying the plasma temperature from 1000 K to 2500 K and the relative concentration of  $0^+$  from 20% to 80%. The extrapolated profiles extend to a height of 4 Earth radii, 4R, the assumed height of the plasmapause. Above that height, the electron concentration was assumed to be zero. Ratios between the computed  $I_w$  and the electron content above a height h,  $I_u = \int_h^{4R} n$  sec  $\chi$  dh, were calculated, the height h ranging from 500 km to 4000 km.

Given a backscatter profile and the plasma temperature, a family of curves  $I_{\rm w}/I_{\rm u}$  vs. height is generated by varying the 0+ relative concentration at the 800 km level. Examples of such families of curves are plotted in Figure 12 for temperatures of 1000 K, 1500 K, and 2500 K. For any height above 800 km and below 4000 km and for a fixed temperature, the 20%

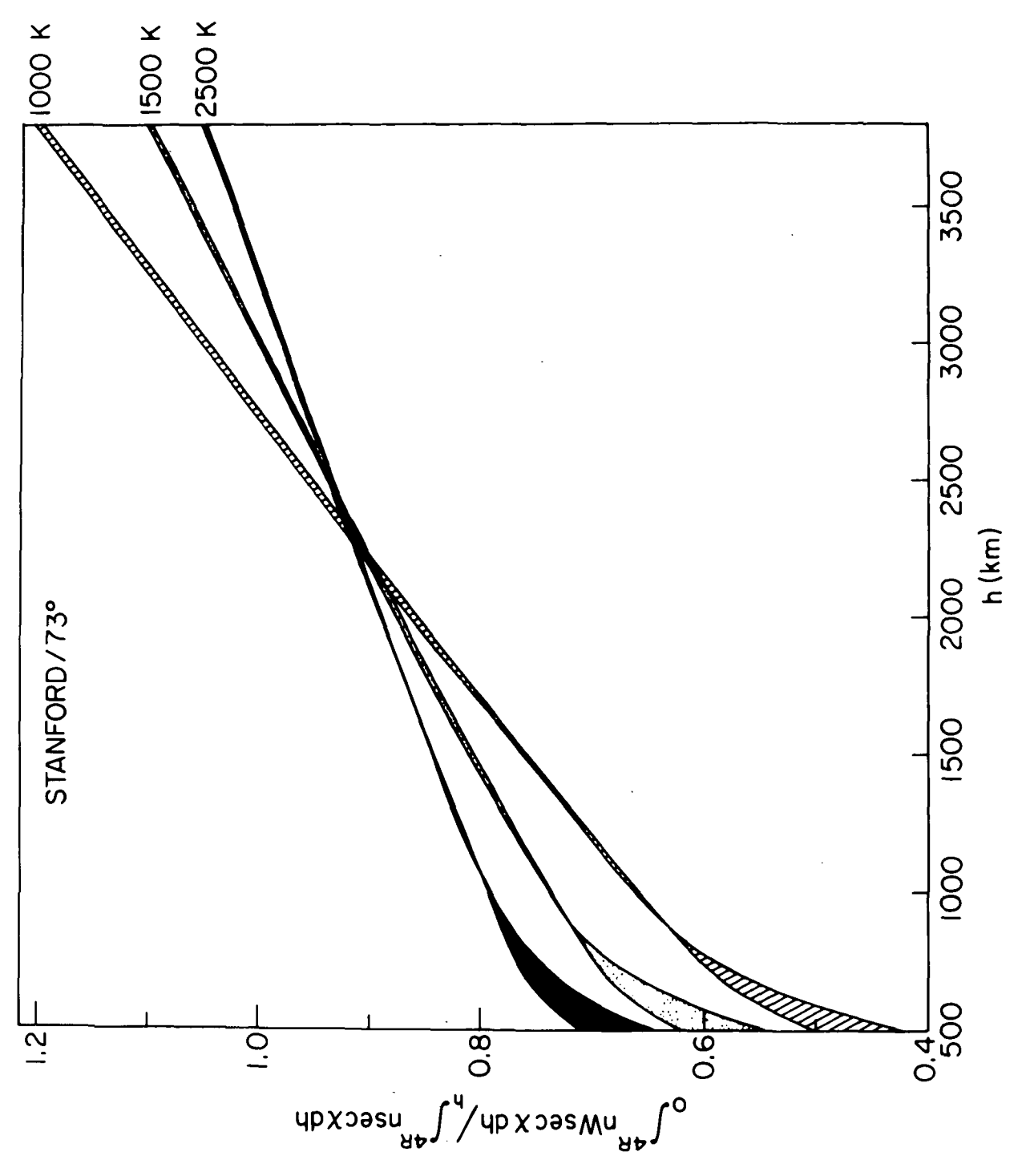


Fig. 12. VARIATION WITH HEIGHT OF THE RATIO BETWEEN THE QUANTITY I AND THE ELECTRON CONTENT ABOVE THAT HEIGHT FOR STANFORD AND A GEOSTATIONARY SATELLITE AT -73° E. Both quantities were computed adopting a representative Each famdaytime ionospheric profile extrapolated to four Earth radii using diffusive equilibrium models. The three families of curves shown correspond to different plasma temperatures (1000 K, 1500 K, and 2500 K). ily was generated by varying the relative concentration of 0+ ions, at 800 km, from 20% to 80%.

to 80% variation in the 0<sup>+</sup> concentration causes a change in the ratio  $I_w/I_u$  which never exceeds 0.02. Changes in temperature are more effective in causing variations in the ratio  $I_w/I_u$ , even though the maximum variation is 0.17 when the temperature is more than doubled.

The more interesting and useful result is that all the families of curves in Figure 12 cross each other at the same height near 2300 km, where the value of the ratio  $I_w/I_u$  is 0.91. The plots of Figure 12 were obtained using a backscatter profile representative of daytime conditions, but almost identical results were obtained for backscatter profiles representative of other hours of the day. The scatter in the values of  $I_w/I_u$  is less than 0.02 and in the height where the curves cross each other is less than 200 km. The assumption of a plausible plasmapause height is not critical. Variations in the height of the plasmapause of  $\pm 1.5$  Earth radii cause fluctuations of  $\pm 0.02$  in the ratio  $I_w/I_u$  and the effect on the height of crossing is negligible.

From the discussion above it follows that as long as the diffusive-equilibrium models are valid approximations, I  $_{\rm W}$  can be interpreted as a measurement of the electron content above 2300 km, for an observer at Stanford and the satellite at -75°  $\pm4^{\circ}$  E .

The above conclusion is of great significance because it opens the possibility of continuous measurement, with excellent time resolution, of the protonospheric columnar content by using a relatively inexpensive technique. Based on the computations made for Stanford and Arecibo, it is expected that given a geostationary satellite position, a midlatitude site can be found such that the resultant geometry is similar to Stanford/73 or Arecibo/122. This makes the use of the Faraday-phase-path difference

technique more attractive for measurement of the electron content of the upper plasmasphere.

# B. Geostationary satellite observations combined with backscatter ionization profiles.

For geometries of the type (a) it has been concluded that the Faraday and phase-path difference data does not contain information enough to permit a reasonable determination of the protonospheric content. Additional information on the bottom side of the ionosphere from ionograms is not enough to solve the problem. The use of backscatter electron concentration profiles can, however, greatly improve the situation.

The shape and height, h  $_{max}$ , of the ionospheric electron concentration profiles from radar backscatter measurements, made simultaneously with Faraday and phase-path difference observations, are the necessary information to determine the values of  $B_{LI}$  which minimize  $I_{w\ell}$ . The time resolution of this combined technique is limited by the integration time, typically of 30 minutes, used to process the radar ionospheric profile data. Such resolution is, however, quite satisfactory for some long term observations. The real great difficulties in the implementation of such combined technique are the high cost of the backscatter profiles and the low availability of radar installations capable of covering the ionospheric heights.

Because the Arecibo radar operations schedule is such that electron concentration profiles are obtained in a regular routine basis, and because the ATS-3 is usually parked around  $-73^{\circ}E$ , it is of interest to interpret the meaning of  $I_{w}$  derived from the combined technique for the geometry Arecibo/73.

Again, using the same procedure adopted for the Stanford/73 case, calculations of the ratio  $I_w/I_H$  were made with the aid of diffusive-

equilibrium profile models for the Arecibo/73 geometry with the difference that now  $B_{LI}$  is not held constant but instead is made to vary in such a way that it assumes the values which minimize  $I_{w\ell}$  for each backscatter profile used in the test.

The results are almost identical to the ones obtained for the Stanford/73 case with the exception that the height where the  $I_{\rm w}/I_{\rm u}$  curves cross each other is near 1700 km and the value of the ratio at that height is 0.95. This conclusion is also of great significance despite the fact that it implies the use of a more expensive operation and the additional complication of dealing with acquisition and processing of the more sophisticated radar data in order to determine the protonospheric content.

There is considerable interest in the simultaneous observation of protonospheric content from sites with local time differences of several hours. For a given satellite position there are only two regions, located at approximately 50 degrees East and West of the satellite position, where the favorable geometry of protonospheric observations occurs.

Of the spacecrafts presently carrying aboard the VHF/UHF pair of beacon frequencies, the ATS-3, because of technical difficulties with ATS-5, is the more suited for the Faraday-phase-path difference experiment. Important scientific and technical considerations require the positioning of ATS-3 around -73°E for long periods of time. This makes Stanford one of the ideal sites for carrying the protonospheric observations. The other lies somewhere in the middle of the Atlantic ocean. The possibility of successful protonospheric observations from a site where the resultant geometry of observation does not conform to (b), but iono-

spheric electron concentration profiles are available, makes Arecibo another possible site for the observations.

# Page Intentionally Left Blank

# CHAPTER IV

# RESULTS

Faraday rotation angle and phase-path difference data (ionospheric Doppler frequency shift) using VHF and UHF signals transmitted from the geostationary satellite ATS-3, were recorded at Stanford and Arecibo.

Very few instances of phase-path difference data covering periods longer than 24 hours with no interruption, were obtained due to the relatively modest antenna gain of 23 dB used to track the dominant spectral component (4.5 mW ERP) of the UHF signal (see Chapter 2). Only the uninterrupted data covering periods of time (over 24 hours) long enough to permit a good determination of the absolute value of columnar electron content were analyzed by the methods described in Chapters 2 and 3. A total of 450 hours of observations were considered in this work.

The Arecibo data, covering a period of 5 days in December 1968 with no interruption, were acquired when the ATS-3 was drifting from -47.4°E to -50°E and correspond to the most unfavorable geometry for determination of protonospheric content by using the Faraday and phase-path difference technique. Ionospheric electron concentration profiles, the additional information necessary for determination of protonospheric content in such case, were not available for that same period of time. Such data are presented here to illustrate the discussions of Chapter 3.

Most of the Stanford data, some 320 hours, were collected when the satellite was parked at  $-73^{\circ}\pm0.5^{\circ}$  E, a situation which corresponds to the most favorable geometry for protonospheric observations by the Faraday-phase-path difference technique.

The Stanford observations cover several days in April and May 1969, a period of time not long enough for a statistical study of the behavior of the protonospheric electron content. Luckily, however, the observations cover geomagnetic activity ranging from very quiet to highly disturbed days when changes in the height of the plasmapause are expected to occur (Carpenter[1966]). Depletion of the plasmasphere following the increase of geomagnetic activity was detected by the corresponding decrease in protonospheric electron content in general agreement with the behavior of tube electron content measured by the whistler technique during a geomagnetic storm (Park[1970]). Of particular interest are the data taken during the storm of May 14, 1969, from Stanford. The behavior of the protonospheric content is consistent with a storm model in which the outer plasmasphere is 'peeled' away by sunward convection and is subsequently replenished by slow filling from the underlying ionosphere (Chappell et al.[1971]).

# A. Arecibo Observations

Approximately 140 hours of uninterrupted phase-path difference and Faraday rotation angle data were obtained at Arecibo from 6 to 11 December 1968. The geostationary satellite ATS-3 was drifting from -47.4°E to -50°E during the period of observation. The resultant geometry of observation is very similar and even less favorable for protonospheric content determination than the one, which corresponds to the satellite positioned at -73°E, studied in Chapter 3. Unfortunately, ionospheric electron concentration profiles which can provide a means of estimating the right values of  $B_{LI}$  which minimize the contribution of the ionospheric electron content to  $I_{\rm w}$ , were not available for that period of time. For

this reason, several derivations of  $I_w$  from the observed data were made each one corresponding to a constant value of  $B_{LI}$ . The values of  $B_{LI}$  used correspond to heights between 300 km and 350 km and should approximately correspond to the bounds of the optimum value of  $B_{LI}$  for such case, as seen in Chapter 3. Figure 13 shows plots of electron content, I, compared to plots of  $I_w$  obtained at Arecibo. The curves of  $I_w$ , in Figure 13, labeled (a) and (b) correspond to values of  $B_{LI}$  computed at heights of 300 km and 350 km, respectively. It can be seen from the figures that  $I_w$ , case (a), strongly correlates with I and that such correlation is much less accentuated for case (b). In both cases  $I_w$  reaches negative values in the early morning of the days 8 and 11. Such behavior of  $I_w$  is entirely consistent with the analysis presented in Chapter 3. Because ionospheric electron concentration profiles were not available, no attempt was made to interpret  $I_w$  in terms of protonospheric content.

A good example of how ionospheric electron concentration profiles can be used to improve the determination of  $I_w$  is the observation made between 29 and 30 January, 1969, during a period of 24 hours when backscatter ionospheric profiles were available approximately at one hour intervals. Figure 14 shows plots of  $I_w$  obtained by assuming a constant value of  $B_{LI}$  (solid line) computed at the height of 350 km which is close to the optimum value for the satellite parked at -73°E, and a plot of the corrected values of  $I_w$  (open circles) derived by using values of  $B_{LI}$  estimated from the shape of the backscatter ionization profile measured at the same time. It can be seen from the figure that the use of a constant value of  $B_{LI}$  yields negative values of  $I_w$  in the middle of

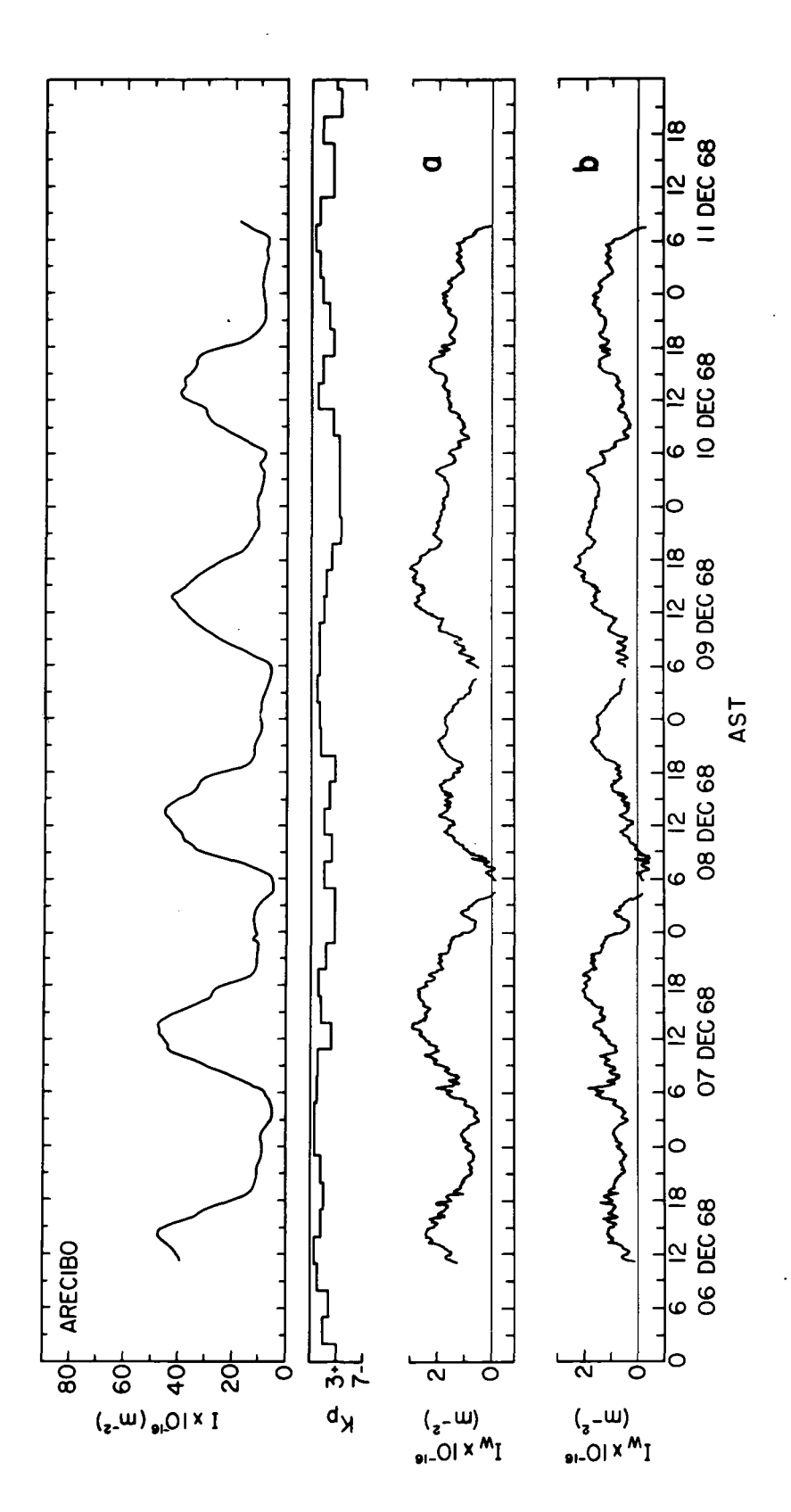


Fig. 13. PLOTS OF TOTAL SLANT ELECTRON CONTENT, I, AND OF THE QUANTITIES I DETERMINED FROM OBSERVATIONS OF ATS-3 AT ARECIBO. The I curves labeled a) and b) were obtained FROM OBSERVATIONS OF ATS-3 AT ARECIBO. The I curves labeled a) and b) wusing constant values of  $B_{LI}$  computed at 300 km and 350 km, respectively.

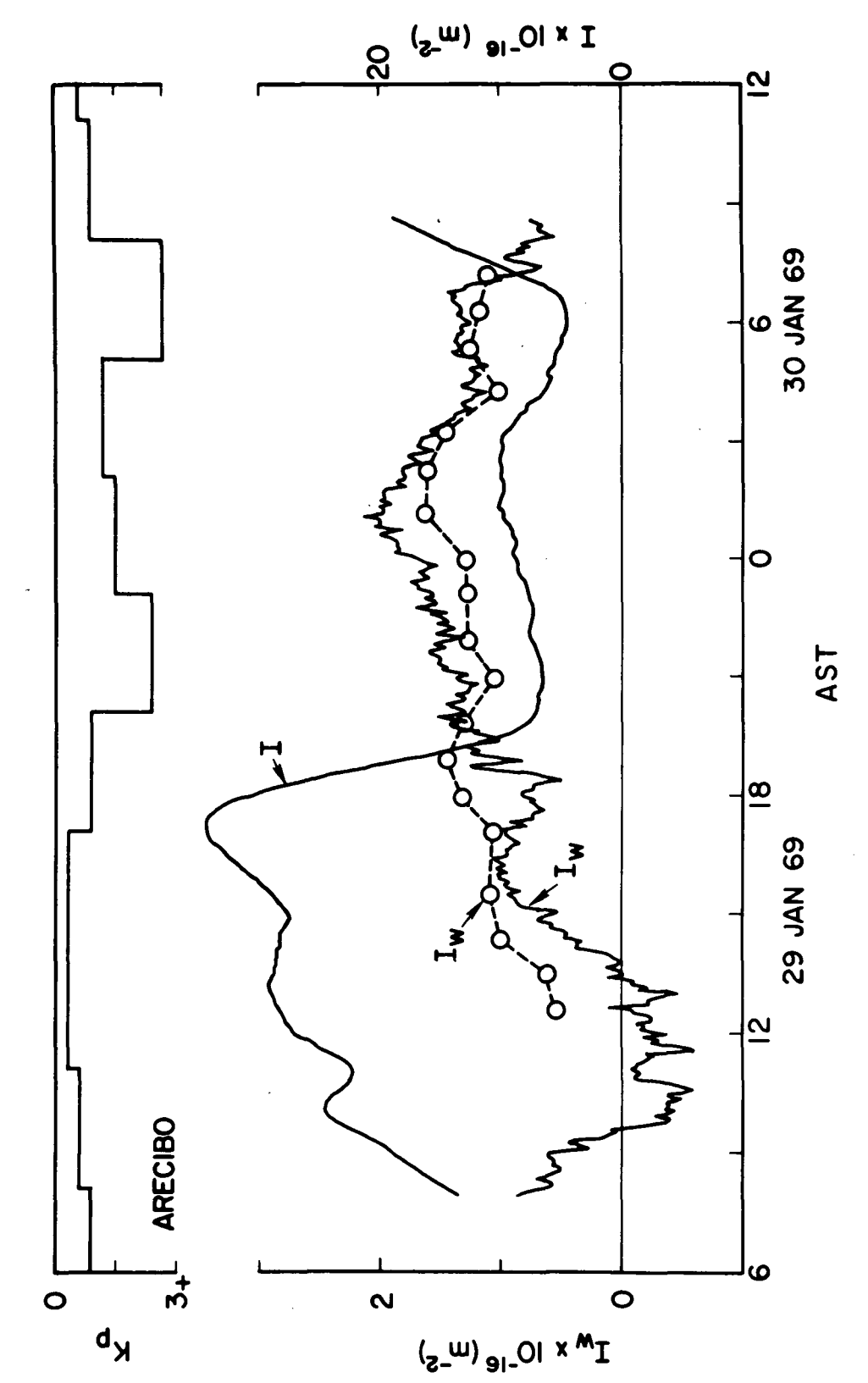


Fig. 14. DIURNAL VARIATION OF PROTONOSPHERIC ELECTRON CONTENT AT ARECIBO. The solid line labeled I was obtained using a constant value of B  $_{\rm LI}$  computed at 350 km. The open circles, connected by dash line, are the values of I  $_{\rm W}^{\rm LI}$  corrected using information on the shape and height of the simultaneously observed backscatter profiles. The total slant electron content (solid trace), I, and the three hour universal geomagnetic index, K, p are also shown.

the day on 29th, values lower than the corrected ones (open circles) by as much as  $0.8 \times 10^{16} {\rm el.m}^{-2}$ . The nighttime values of both corrected and not corrected I are in relatively good agreement.

During the geomagnetically quiet period of 29 to 30 January, the protonospheric electron content, the corrected I ,, increased during the day probably due to ionospheric flux into the protonospheric region, leveled off around sunset time and stayed nearly constant during the night. A decrease in the protonospheric content was not detected during the night of 29th to 30th being probably masked by the irregularity (bump) observed in the total electron content, I, also shown in Figure 14, which is coincident with a small 'bump' seen in the protonospheric content, indicating that such irregularity extended to higher altitudes. The other 'bump' observed around local sunset with a peak occurring at about 19 LT could possibly be interpreted in terms of an increase in the content corresponding to the passage of the observer-to-satellite path through the plasmasphere bulge. It should be emphasized here that no attempt has been made to definitely establish the origin of the observed irregularities because this was the only case in which protonospheric content measurements were made at Arecibo. The observed features should be extensively studied when more data become available.

## B. Stanford observations during the magnetic disturbed period of 12 to 18 May 1969.

Uninterrupted measurements of Faraday rotation angle and differential phase-path data were made at Stanford when the geostationary satellite ATS-3 was parked at -73.4°E, covering the period starting at 0500 UT on 12 May and ending at 0130 UT on 19 May 1969. Very high quality data

were obtained during that period and, because the geometry of observation was very favorable, the quantity  $\mathbf{I}_{\mathbf{W}}$ , resulting from the combination of the Faraday and phase path data, could be interpreted in terms of protonospheric electron content. It was the first time continuous experimental determination of the columnar electron content of the upper plasmasphere covering a period of more than 6 days has been made.

The relative variations of the observed  $I_w$  are very accurate and the error in the absolute level of  $I_w$  is estimated to be  $\pm$  0.5 x  $10^{16} {\rm el.m}^{-2}$  which is less than 13% of the maximum observed value of  $I_w$  during the period in question. The uncertainty that has to be assigned when  $I_w$  is interpreted in terms of protonospheric content above a certain level, is not precisely known because it depends on the shape of the ionization profile above the ionosphere, say above 1000 km. If diffusive equilibrium ionization distribution models are adopted,  $I_w$  is a measure of 90% of the electron content above the level of 2300 km and, based on the analysis of the previous chapter, the uncertainties involved in such interpretation are much smaller than the error in the absolute value of  $I_w$ . It is our belief that a total uncertainty of  $\pm$  20% could conservatively be assigned to the interpretation of  $I_w$  as the columnar electron content above the level of 2300 km.

The period preceding the beginning of observations was generally quiet and the day before 12 May was very quiet, with  $K_p$  never exceeding 2. On the 12th, at about 0900 PST, a period of moderately to highly disturbed geomagnetic activity starts, and extends to 1130 PST on 14 May when an SSC occurs which is followed by a storm during which  $K_p$  had returned to a level lower than the one which preceded the SSC. On the 17th, at

63

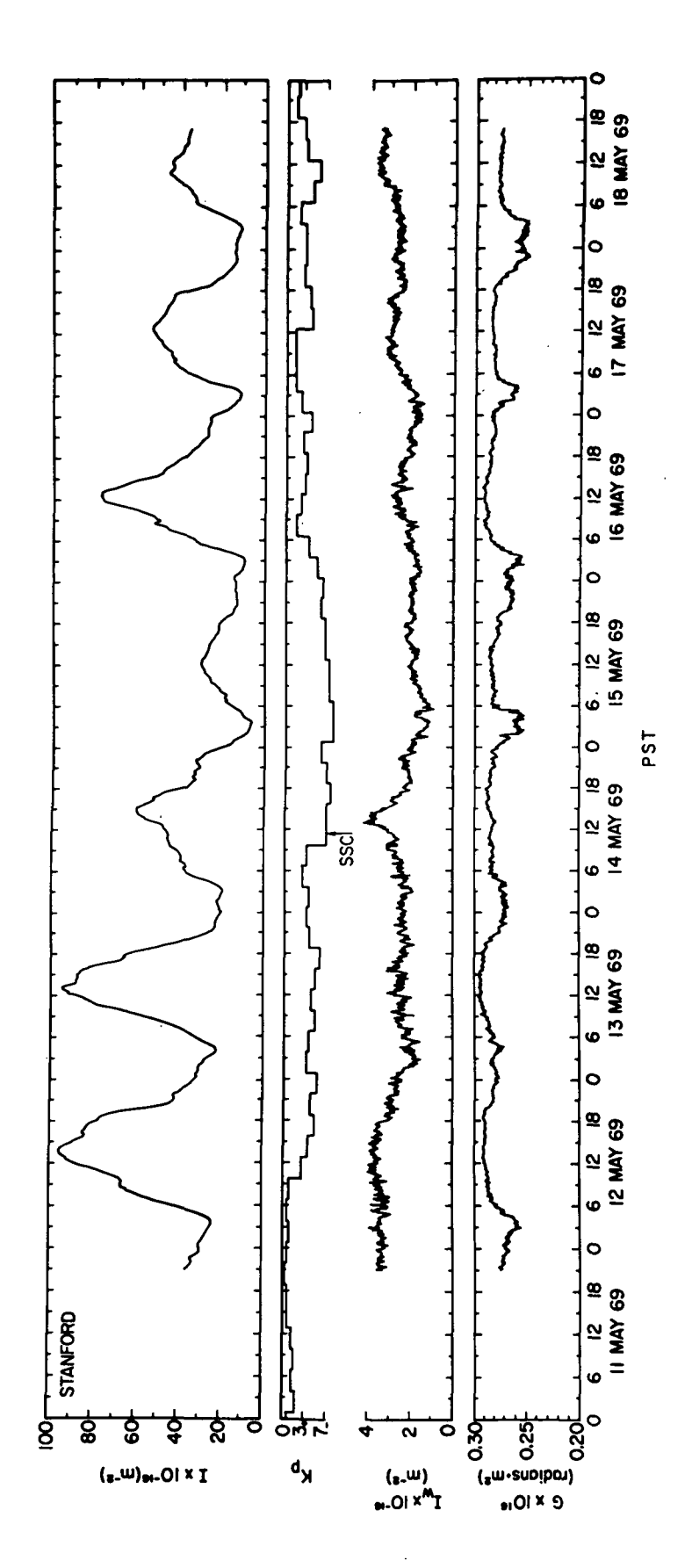


Fig. 15. PROTONOSPHERIC ELECTRON CONTENT OBSERVATION, DURING AN UNINTERRUPTED PERIOD OF 7 DAYS IN MAY 1969, FROM STANFORD. The geostationary satellite was parked at -73.4° E.

around 1200 PST, a period of moderate activity starts to develop extending through 1500 PST on the 18th when the protonospheric observations were interrupted. The above feature of the geomagnetic events ranging from very quiet to highly disturbed affords a somewhat rare opportunity of observing the behavior of the columnar electron content of the upper plasmasphere during a period in which almost extreme magnetic conditions were present.

Plots of total electron content, I, protonospheric electron content,  $I_w, \ \ \text{the parameter G, and the universal geomagnetic index K}_p, \ \ \text{versus}$  time during the period in consideration are shown in Figure 15.

Because the ionosphere contributes some 90% or more to the total electron content, the values of I reflect predominantly the behavior of the ionospheric content near Stanford. It should be pointed out that I is the total electron content along the observer-to-satellite path, also denoted as 'total slant electron content', measured by the differential phase-path technique.

On 12 May the electron content reached a maximum of 96 x 10<sup>16</sup>el.m<sup>-2</sup> during the day comparable to the maximum observed on the next day, 13 May, when the increase in geomagnetic activity had already persisted for more than 24 hours. Only on 14 May are the effects of the increase in the disturbances detectable in the depressed content of the ionosphere.

After the occurrence of the Sudden Storm Commencement (SSC) at 1129 PST on 14 May, the content exhibited an increase with a maximum at 1500 PST. The next day, 15 May, the ionospheric content is strongly depressed.

One can see the effect of increased magnetic disturbances on the protonospheric content,  $I_{w}$ , in the night of 12 to 13 May following the

beginning of the disturbed period. It should be remembered here that the local time at the satellite is about 3 hours later than the local time at the observer site. A gradual reduction in the protonospheric content is observed after 1800 PST on the 12th, and the content levels off at satellite dawn on the 13th and stays nearly constant throughout the day. The observed reduction in protonospheric content is interpreted as a shrinking of the plasmasphere as the plasmapause boundary moves inward during the night sector where convection effects are important, and a corresponding plasma loss. Determination of the plasmapause positions by the Lockheed light-ion mass spectrometer on OGO-5 at L = 6.5 around 1130 LT (2230 UT) on 12 May during the inbound pass and at L = 5 around 2000 LT (2350 UT) on the same day during the outbound pass, (Chappell, C.R., private communication), are in agreement with our protonospheric observations covering the same period.

On 12 May, the daytime protonospheric content stays at the same level observed prior to the onset of the disturbed period, and is an indication of the inability of the dayside plasmasphere to quickly respond to changes in magnetic activity. Such observed behavior supports suggestions made by Carpenter et al.[1969] and Chappell et al.[1970], that the position of the plasmapause on the dayside sector is dependent on the magnetic activity present at the time the sector in question corrotated previously through the nightside.

On 14 May, a sharp increase in the protonospheric content is observed following the 1929 UT SSC. The increase lasts for some 2.5 hours and then  $I_{\overline{W}}$  decreases below the level existing prior to the storm commencement. The protonospheric content levels off around satellite dawn, on

the 15th, and stays nearly constant throughout the rest of the day. Again the OGO-5 measurements indicate that the L shell value of the plasmapause position is slightly below 3 around 1900 LT (1400 UT) a fact that is in agreement with the additional reduction of the protonospheric content observed at the nightside sector following the onset of the storm. The sudden increase in protonospheric content observed during the day, 30 minutes after the SSC, is probably linked to the sunward motion of the plasma set up by an increase in the convective electric field and will be studied in more detail in the next section.

The reduction of the protonospheric content following the increase in the magnetic disturbances is observed to start after the satellite has passed the dusk meridian and ends when the satellite has passed the dawn meridian during the period 14 to 15 May. Such behavior, again, is in agreement with the hypothesis that the plasmapause position is determined by magnetic conditions present during the time the plasmasphere sector corrotates through the nightside.

The protonospheric content stayed about the same depressed level throughout the 15th, and the geomagnetic activity persisted in the same level during that period. From 16 to 18 May, when the level of the magnetic activity decreases, the plasmasphere is subsequently replenished by slow filling from the underlying ionosphere. The relative rate of protonospheric content recovery during that period is  $(\Delta I_w/I_w) = 1.0$ . Based on observations of electron content recovery of a tube of flux at L=4 made by the whistler technique following the storm of 15 June 1965  $(\underline{Park}[1970])$ , the relative rate of recovery during the first 3 days is  $(\Delta I_w/I_w) = 1.2$ . The agreement between the protonospheric content and the

tube flux content recovery rates is excellent despite the fact that the observations were made almost at opposite extremes of the solar activity cycle.

Plots of the parameter G are also shown in Figure 15 for the sake of completeness. It can be seen that the daytime values of G, during the period of observation, vary from day to day by as much as 5%.

### C. Protonospheric content observations during magnetic storms.

The dynamic behavior of the plasmapause has been the subject of many investigations. Although the basic convection model proposed by Axford and Hines[1961] is generally accepted, there is no definitive explanation for the way the plasma escapes from the plasmasphere following an enhancement of the geomagnetic activity.

Sunward surges of plasma in the magnetosphere, detected by the whistler technique, in the evening sector of the plasmasphere, that appear to be associated with substorm activity have been reported by Carpenter [1970]. Measurements of mass of plasma detached from the main body of the plasmasphere following periods of moderate to high magnetic activity, indicate that such detachments tend to occur more often in the afternoon-dusk sector of the plasma trough (Chappell et al.[1971]). Such observations seem to suggest that the plasmasphere is peeled away by sunward convections of the plasma.

Using an extension of the magnetospheric convection model suggested by Axford and Hines[1961], Carpenter[1962], Nishida[1966], and Brice[1967], Chappell et al.[1971] have demonstrated qualitatively that as the convection electric field increases, following the increase in magnetic activity, the dayside flux tubes are convected toward the magnetopause. The corresell-72-019

sponding convection flow diagram is such that the flow lines are almost perpendicular to the plasmasphere surface in the afternoon-dusk sector. This flow pattern implies that the tubes of plasma are carried away from the plasmasphere, peeling off the outer plasmasphere in a sunward direction and that the process is more effective in the afternoon-dusk sector where the flow lines tend to converge.

Observations of protonospheric electron content using geostationary satellites provide a way of continuously monitoring the same region of the plasmasphere. Because the plasmasphere, except during very quiet magnetic periods, normally extends up to around 3 Earth radii (L=4), the protonospheric content measurements using geostationary beacons orbiting at 5.6 Earth radii (L=6.6), reflect the total content of the upper plasmasphere. Such protonospheric observations may also detect large radial movements of plasma, especially sudden outward motions as the kind expected following large enhancements of magnetic activity. These movements reveal themselves as increases in the protonospheric content, provided such surges of plasma originate at heights lower than the geostationary orbit, say 3 to 4 Earth radii.

Measurements of protonospheric electron content were made at Stanford during the storms of 27-28 April 1969 and 14-15 May 1969. The period of 24 hours that preceded both storms was moderate in one case, and highly disturbed in the other. Thus, based on the experience accumulated of plasmapause position measured by the whistler technique, the plasmapause can be estimated to be positioned at L values of 3 to 4 right before the onset of the storms.

The storm of 27-28 April was preceded by an SSC that occurred on

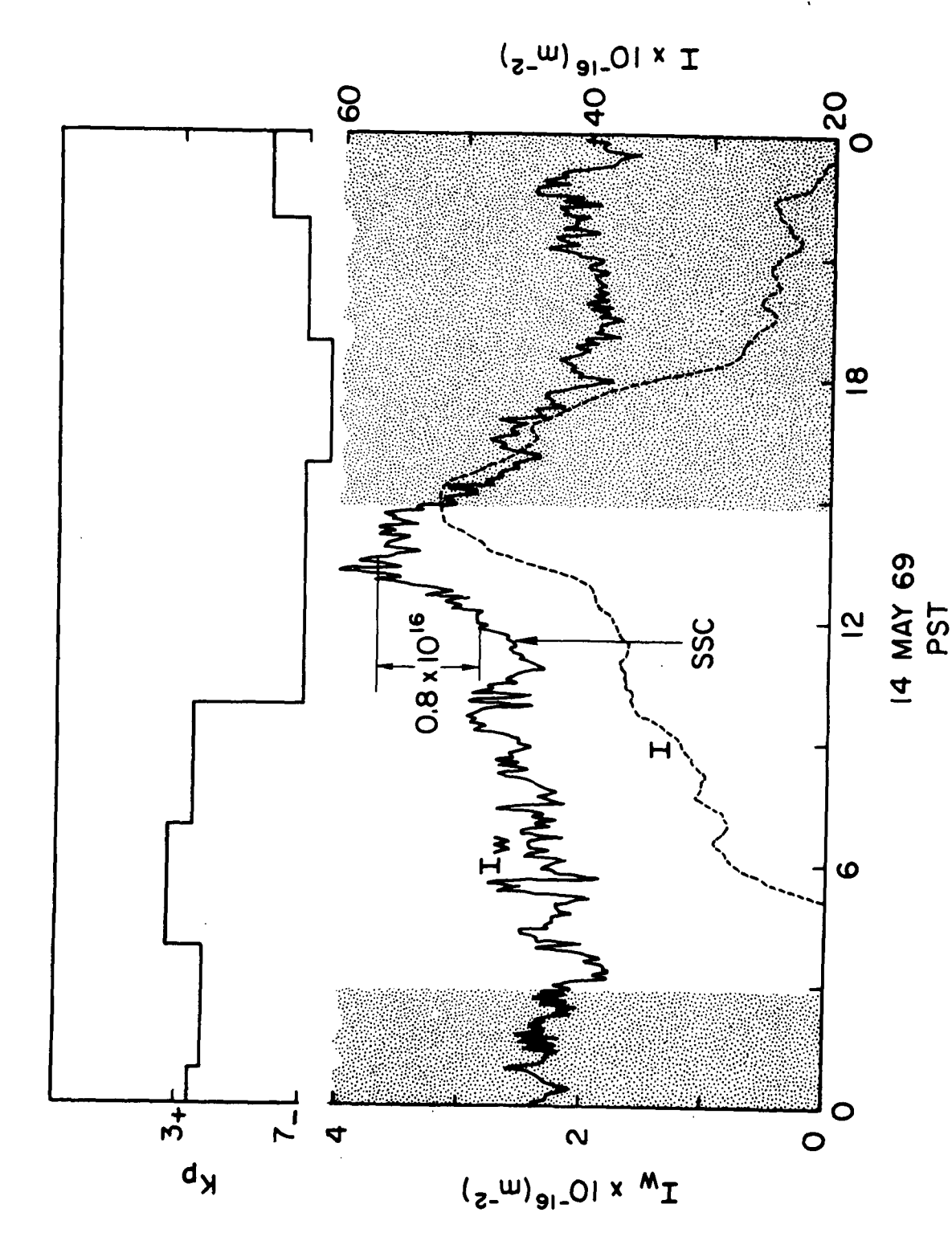
the 28th at 0252 UT, 2200 LT on the previous day at the ATS-3 satellite. The protonospheric content following the onset of the magnetic disturbances gradually decreased during the night leveling off around satellite dawn. This behavior is consistent with the storm-time model (Chappell et al.[1971]) discussed above, which predicts always inward motion of the tubes of plasma on the nightside.

The storm of 14-16 May followed an SSC which occurred on the 14th at 1929 UT, 1430 LT at ATS-3, exactly when the satellite was entering the afternoon-dusk sector. The universal three hour geomagnetic index,  $K_p$ , jumps from 4- to 7- following the onset of the storm.

The protonospheric content,  $I_w$ , starts increasing right after the SSC, as can be seen from Figure 16, reaching a maximum 1.5 hours after the event. This maximum level is maintained for 2 hours, and then  $I_w$  starts to decrease very fast around 1500 PST when the satellite is entering the nightside sector. During this time the protonospheric content reached a maximum level nearly equal to the one observed on 12 May when the plasmapause was at L=6.5.

The observed sudden increase in  $I_w$  cannot be explained by errors introduced by the elimination of the ionospheric content neither by changes in the longitudinal component,  $B_L$ , of the geomagnetic field, associated with the storm.

Very drastic changes in the shape and height of the ionospheric concentration profile may occur during a storm. Such fluctuations could be in the direction to increase the contribution of the ionospheric content to the measured  $I_w$ . An estimate of the error in  $I_w$ , associated with the possible changes, was made based on profiles, extending up to 1000 km, in



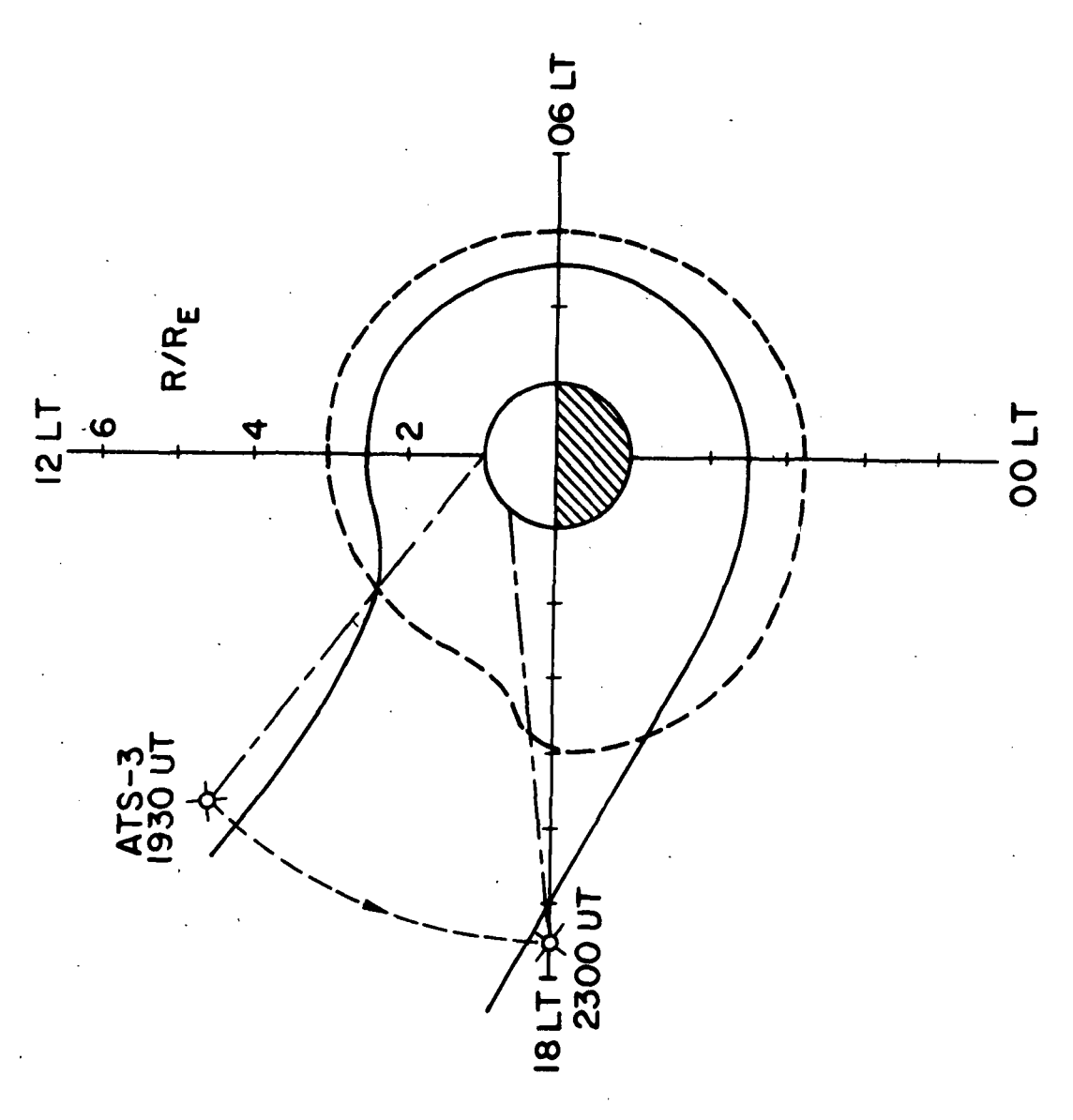
trace curve, I , is the observed electron content of the protonosphere. The total slant electron content (dash trace), I, and the universal geomagnetic index, K , The solid are also shown. The shaded region in the figure corresponds to the geostationary Fig. 16. PROTONOSPHERIC ELECTRON CONTENT ON 14 MAY 1969, FROM STANFORD. satellite ATS-3 corrotating in the nightside.

which the shape and height were varied but the content was kept constant and equal to  $45 \times 10^{16} \, \mathrm{el.m}^{-2}$ . The computations indicate that for that particular geometry of observation, increases in height are more effective than changes in the shape of the ionospheric layer in increasing the error, even though an increase of 200 km in h can account for a change of only  $10^{15} \, \mathrm{el.m}^{-2}$  in  $I_{\mathrm{w}}$ .

Fluctuations of the horizontal component of the geomagnetic field associated with the storm cause changes in  $B_L$ . The resulting variations of the values of the weight function  $W=(1-B_L/B_{LI})$ , see Chapter 3, introduce fluctuations in  $I_w$ .

The increase of  $I_w$  was observed during the initial phase of the storm, when percentually small enhancements of the horizontal component were observed at the earth's surface. At low L values the increase in the horizontal component causes an increase in  $B_L$  which corresponds to a decrease in  $I_w$ . At higher L values the above mentioned component may decrease by a factor of two but  $B_L$  is primarily determined by the vertical component. Even if an absurd decrease of  $B_L$  by a factor of two is adopted, the corresponding change in W is of the order of 4% (even less for L values higher than 4) and cannot explain the detected 27% increase in  $I_w$ .

A plausible explanation for the observed increase in  $I_w$ , consistent with the storm-time model mentioned previously, is that storm induced enhancement of magnetospheric electric fields cause large masses of plasma to be convected outwards around both sides of the planet converging in the afternoon-dusk sector in an 'outflow lane' as depicted qualitatively by the solid lines in Figure 17. This figure represents the equatorial plane of Earth. When the observer-to-satellite line sweeps through the



line corresponds to an idealized plasmapause shape before the onset of the 14 May 1969 storm. The solid line observer points, on the plane, are also shown. The numbers by the satellite give the universal time at those is a possible picture of the plasmapause after the onset of the storm. The projections of the satellite and Fig. 17. QUALITATIVE PICTURE OF THE SHAPE OF THE PLASMAPAUSE TRACE ON THE EARTH'S EQUATORIAL PLANE. The dash positions,

sector containing the outflow lane, a much larger protonospheric electron content is measured. The SSC occurred when the satellite was either inside or about to enter the 'then empty' outflow lane so that a time interval of about 1.5 hours elapsed during which the plasma front moved outward to the satellite height. During this period, the observed protonospheric content increased. Once the front was beyond the satellite height, the content remained fairly constant for about 2 hours until the observer-to-satellite line started leaving the lane. As ATS-3 moves into the nightside sector, the expected fast decrease in the protonospheric content is observed.

The interpretation of the  $\mathbf{I}_{\mathbf{W}}$  behavior offered above implies the existence of an electric field associated with the storm given by the hydromagnetic relation.

$$\overrightarrow{E} = \overrightarrow{-v} \times \overrightarrow{B}$$

or

$$\overrightarrow{v} = \frac{\overrightarrow{E} \times \overrightarrow{B}}{\cancel{B}^2}$$

where  $\overrightarrow{v}$  is the plasma drift velocity and  $\overrightarrow{B}$  the geomagnetic field.

Unusually large westward plasma drifts detected by the incoherent scatter radar technique at ionospheric heights (about 250 km) on May 14 are consistent with the hypothesis of existence of electric fields in the magnetosphere (Evans[1972]). Observations at Millstone Hill showed that the horizontal drift velocity, right after the SSC, became much larger than normal and was directed toward the west. The northward directed electric field associated with the 200 m.s $^{-1}$  drift velocity observed, is of the order of 10 mV.m $^{-1}$ . Such field maps at the top of the flux tube (L = 3.3) on the equatorial plane, with intensity of the order

of 1 mV.m<sup>-1</sup> and directed radially outward. This component alone could explain surges of plasma, coming from the bulge region (evening region), convecting in a westward direction (zero radial velocity) with the tip of the bulge advancing faster because the drift velocity varies with the cube of the geocentric distance. Although the above picture could qualitatively explain an increase in protonospheric content it is not very attractive because during the previous sweep of the observation path (observer-to-satellite line) through the bulge region, on May 13, the observed protonospheric content was depressed (see Figure 15) to a level much lower than the one observed when the plasmapause was at L=6.5. on the 12th. Therefore, the bulge region was not likely to extend to high L values. Moreover, there should not be a reason for a preferential direction of the electric field associated with the magnetic disturbances. It is plausible to admit also an east-west component of the convective electric field,  $\mathbf{E}_{o}$ , which can set up radial drift velocity thus moving the flux tubes of plasma in an outward direction. Such east-west component mapped in the ionosphere would cause vertical drifts of plasma and a rapid increase in  $h_{\text{max}}$ . The ionization layer is therefore moved to higher levels where the losses are less and enhancements of  $n_{\text{max}}$ , the electron concentration maximum, would follow. Evans[1970], reported that during the June 1965 magnetic storm, the height of the layer, h began to increase in the early afternoon of 16 June and that the large observed increase in  $\boldsymbol{n}_{\max}$  was associated and probably caused by the large increase in  $h_{\text{max}}$ . Furthermore, the east-west electric field intensity that would establish drift velocities capable of producing a rapid change in the layer height, was roughly estimated to be 5 mV.m<sup>-1</sup>.

An estimate of the east-west component of the convective electric field,  $E_{\phi}$ , consistent with the storm-time behavior model was made based on the following assumptions: 1) the  $E_{\phi}$  field is uniform, 2) the geomagnetic field is given by the dipolemodel  $B=B_0L^{-3}$ , where  $B_0$  is the intensity on the Earth's surface, 3) the time,  $\Delta t$ , it takes for a representative particle to move radially from the neighborhood of the plasma-pause to the satellite height is equal the time elapsed between the SSC and the moment when the protonospheric electron content first reached its maximum (1.5 hours), and 4) the observer-to-satellite path at heights above L=3 is on the geomagnetic equator. Under the above conditions,  $E_{\phi}$  is given by

$$E_{\varphi} = \frac{B_0 R}{2\Delta t} (L_p^{-2} - 2.296 \times 10^{-2})$$

where R is the Earth radius and L  $_{p}$  the average plasmapause position prior to the SSC event.

Now, if one assumes  $L_p$  to be 3.5 (a very plausible value based on the level of the magnetic activity present at the time) then the estimated value of  $E_{\dot{\phi}}$  is 1 mV.m<sup>-1</sup>. Estimates of convection electric field strength in the dusk magnetosphere during substorms, made by <u>Carpenter</u>[1970], indicate values of the order of 1 mV.m<sup>-1</sup>.

Our estimated east-west electric field maps in the ionosphere near Millstone Hill (L = 3.3) with an intensity of 6 mV.m $^{-1}$  which is the same order of the east-west electric field, estimated by  $\underline{\text{Evans}}[1970]$ , associated with the enhancements of h and n observed during the June 1965 storm.

The observed increase of I, see Figure 16, when the ionosphere near

Stanford is in the afternoon-dusk sector is consistent with an east-west electric field impressed in the F region by the magnetosphere.

# Page Intentionally Left Blank

### CHAPTER V

#### CONCLUSIONS

The main purpose of this work was to develop a technique of measuring the columnar electron content of the protonosphere making use of the Faraday polarization changes and phase-path length reduction effects observed on the VHF and UHF signals transmitted from the geostationary satellite ATS-3.

The signals received at ground had previously traversed the protonosphere and ionosphere regions. Because the Faraday rotation angle and phase-path length reduction are integral effects, the data used contain information of both, ionosphere and protonosphere, electron contents. The Faraday rotation effect which is related to the product of electron concentration by the geomagnetic field is more sensitive to ionization changes at lower heights and therefore is more determined by the ionospheric content. The phase-path length data, on the other hand, is equally sensitive to ionization changes occurring at any height along the path, therefore, contains integral information on the total content (ionospheric plus protonospheric contents) up to the satellite height.

Earlier attempts to derive the protonospheric content by a suitable subtraction of the electron content, derived from the Faraday data, from the total content derived from the phase-path difference data, have been made by either using lunar radar echoes or satellite transmissions (see Chapter 3 for references). The quantity  $\mathbf{I}_{\mathbf{W}}$ , resulting from the above difference between two large quantities, may be strongly contaminated by the ionospheric content. The difficulty arises from the fact that the

ionosphere contributes some 90% of the information in the data. In order to properly interpret  $\mathbf{I}_{\mathbf{W}}$  as a measure of electron content of the protonosphere, very accurate determinations of the absolute value of the total electron content must be used in the derivation of such quantity, and the ionospheric content contamination in  $\mathbf{I}_{\mathbf{W}}$  must be minimized to a degree reasonably lower than the values of the protonospheric content.

Although, in the mentioned previous efforts, the authors tried to determine only the variations of the protonospheric content, the so called 'relative protonospheric content', thus avoiding the problem of accurate determination of the total content, they failed in properly accounting for the ionospheric content contamination in  $I_{\rm m}$ .

One of the contributions of the present research was the development of a technique of combining the Faraday rotation angle and phase-path difference data to determine the absolute value of the total columnar electron content with uncertainty at least one order of magnitude lower than that of any other existing method (see Chapter 2). The accuracy achieved in such determination is high enough for good determination of absolute values of protonospheric content.

A better understanding of the meaning of the quantity  $I_w$  was gained from the critical analysis presented in Chapter 3. The contamination of ionospheric content in  $I_w$  is dependent on the type of  $B_L$  (longitudinal component of the geomagnetic field) distribution along the path of observation. It was demonstrated that good determination of protonospheric content is only possible for certain geometries of observation such as, for instance, observer at Stanford and the satellite parked at -73° E. For such geometries, the interpretation of  $I_w$  in terms of the columnar

electron content of the protonosphere was discussed based on diffusive equilibrium models of the field-line ionization distribution (Angerami [1966]). Even allowing reasonably large variations of the parameters which determine the ionization profiles, the striking conclusion is that  $\mathbf{I}_{\mathbf{w}}$  reflects 90% of the electron content above 2300 km. However, given a satellite position there are two regions, at midlatitudes, displaced by about  $\pm$  50° in longitude from the satellite, from where good protonospheric observations can be made by the Faraday-phase-path difference technique. For the other geometries, such as Arecibo and the satellite at -73° E, information on the shape and height of the ionospheric layer is necessary to improve the minimization of the ionospheric contamination in  $\mathbf{I}_{\mathbf{w}}$ . Such additional information can be obtained at sites where VHF radar installations are available.

The technique of measuring the columnar electron content of the protonosphere up to the geostationary satellite height developed in this work provides a way of continuously monitoring the same region of the plasmasphere, and is the only one available at present. Because the plasmapause is normally positioned around L=4, except during geomagnetically very quiet periods, protonospheric electron content observations, using geostationary beacons (L=6.6) reflect the total content of the upper plasmasphere.

The protonospheric content observations made during the geomagnetic storms of 27-28 April 1969 and 14-16 May 1969 from Stanford (see Chapter 4) are an example of the new important information that the technique developed in this research brings to magnetospheric investigations. The behavior of the protonospheric content is consistent with a convective

storm model, suggested by Chappell et al.[1971], in which the outer plasmasphere is 'peeled' away by sunward convection and is subsequently replenished by slow filling from the underlying ionosphere.

Of particular interest are the data taken during the storm of 14 May. A sharp increase of the protonospheric content, on the 14th, was observed right after the 1929 UT SSC, and lasted for some 3 hours. During this period the satellite was corrotating from the 1500 LT to the 1800 LT meridians. As the satellite enters the nightside sector of the plasmasphere the protonospheric content starts to decrease very fast. The maximum level reached during the increase of the protonospheric content is nearly equal to the one observed on 12 May when the plasmapause was positioned around the geostationary height.

A plausible explanation for the observed increase in I<sub>w</sub>, consistent with the storm model mentioned above, is that storm induced enhancements of magnetospheric electric fields modify the plasma flow pattern such that large masses of plasma are carried away from the plasmasphere in a sunward direction. Evidence of significative electric fields in the magnetosphere are the unusually large horizontal drifts directed westward observed at Millstone Hill, at that same time, (Evans[1972]). The north-south component of the electric field associated with the observed 200 m.s<sup>-1</sup> drift velocity, corresponds to radially outwards directed component of magnetospheric electric fields of the order of 1 mV.m<sup>-1</sup>. Such a component maps in the ionosphere with intensity of the order of 6 mV.m<sup>-1</sup> and is consistent with the observed increase of electron content in the ionosphere in the afternoon-dusk sector.

Our technique of protonospheric continuous observations can give

detailed accounts of the upper plasmasphere content behavior during geomagnetic storms. Studies of the local time dependence of such stormtime behavior may provide important clues on the magnetospheric convection. REFERENCES

- Almeida, O.G., O.K. Garriott and A.V. da Rosa, Determination of the columnar electron content and the layer shape factor of the plasmasphere up to the plasmapause, Planet. Space Sci., 18, 159, 1970.
- Angerami, J.J., A whistler study of the distribution of thermal electrons in the magnetosphere, <u>Tech. Rept. SEL-66-017</u>, Radioscience Lab., Stanford Electronics Labs., Stanford University, Stanford, California, May 1966.
- Axford, W.I., and C.O. Hines, A unifying theory of high-latitude geophysical phenomena and geomagnetic storms, Can. J. Phys., 39, 1433, 1961.
- Axford, W.I., Magnetospheric convection, Rev. Geophys., 7, 421, 1969.
- Brice, N.M., Bulk motion of the magnetosphere, <u>J. Geophys. Res.</u>, <u>72</u>, 5193, 1967.
- Browne, I.C., et al., Radio echoes from the moon, Proc. Phys. Soc. London, 69B, 901, 1956.
- Budden, K.G., Radio Waves in the Ionosphere, Cambridge University Press, London, 1961.
- Cain, J.C., and R.E. Sweeney, Magnetic field mapping of the inner magneto-sphere, J. Geophys. Res., 75, 4360, 1970.
- Carpenter, D.L., The magnetosphere during magnetic storm, <u>Tech. Rept. SEL-62-059</u>, Radioscience Lab., Stanford Electronics Labs, Stanford University, Stanford, California, 1962.
- Carpenter, D.L., Whistler studies of the plasmapause in the magnetosphere-1. Temporal variations in the position of the knee and some evidence of plasma motions near the knee, J. Geophys. Res., 71, 693, 1966.
- Carpenter, D.L., C.G. Park, H.A. Taylor, Jr., and H.C. Brinton, Multiexperiment detection of the plasmapause from EOGO satellites and Antarctic ground stations, J. Geophys. Res., 74, 1837, 1969.
- Carpenter, D.L., Whistler evidence of the dynamic behavior of the duskside bulge in the plasmasphere, J. Geophys. Res., 75, 3837, 1970.
- Chappell, C.R., K.K. Harris and G.W. Sharp, A study of the influence of magnetic activity on the location of the plasmapause, J. Geophys. Res., 75, 50, 1970.
- Chappell, C.R., K.K. Harris and G.W. Sharp, The dayside of the plasma-sphere, J. Geophys. Res., 76, 7632, 1971.
- da Rosa, A.V., Thermal behavior of the ionosphere and observations of the exosphere and the ionosphere by means of distant earth satellites, Tech. Rept. 2, Radioscience Laboratory, Stanford University, Stanford, California, 1965.

- da Rosa, A.V., and O. Almeida, The ATS protonosphere experiment, NASA

  Quarterly Progress Report, Radioscience Laboratory, Stanford University

  Stanford, California, April 1968.
- de Mendonça, F., Ionospheric electron content and variations measured by Doppler shifts in satellite transmissions, <u>J. Geophys. Res.</u>, <u>67</u>, 2315, 1962.
- Evans, J.V., The June 1965 magnetic storm: Millstone Hill observations, J. Atmos. Terr. Phys., 32, 1629, 1970.
- Evans, J.V., Incoherent-scatter observations of horizontal drifts in the E and F regions of Millstone Hill, presented at the 1972 Spring Meeting of the U.S. National Committee of URSI, Washington, D.C., April 1972.
- Garriott, O.K, The determination of ionospheric electron content and distribution from satellite observations. Part 1. Theory of the analysis, J. Geophys. Res., 65, 1139, 1960.
- Garriott, O.K., and F. de Mendonça, A comparison of methods used for obtaining electron content from satellite observations, <u>J. Geophys. Res.</u>, 68, 4917, 1963.
- Garriott, O.K., A.V. da Rosa, and W.J. Ross, Electron content obtained from Faraday rotation and phase-path length variations, <u>J. Atmos.</u> Terr. Phys., 32, 705, 1970.
- Howard, H.T., B.B. Lusignan, P. Yoh, and V.R. Eshleman, Radar doppler and Faraday polarization measurements of the cislunar medium during the July 20, 1963, solar eclipse, <u>J. Geophys. Res.</u>, <u>69</u>, 540, 1964a.
- Howard, H.T., P. Yoh, and V.R. Eshleman, Radar doppler measurements of the cislunar medium, <u>J. Geophys. Res.</u>, <u>69</u>, 535, 1964b.
- Howard, H.T., Cislunar electron content as determined by radar group delay measurements, J. Geophys. Res., 72, 2729, 1967.
- Jensen, D.C., and J.C. Cain, An interim geomagnetic field, <u>J. Geophys. Res.</u>, 69, 3568, 1962.
- Lorentz, H.A., The theory of electrons, Dover Publications, New York, 1952.
- Nishida, A., Formation of plasmapause, or magnetospheric plasma knee, by the combined action of magnetospheric convection and plasma escape from the tail, J. Geophys. Res., 71, 5669, 1966.
- Park, C.G., Whistler observations of the interchange of ionization between the ionosphere and the protonosphere, J. Geophys. Res., 75, 4249, 1970.
- Ratcliffe, J.A., The Magneto-Ionic Theory and its applications to the ionosphere, Cambridge University Press, 206, 1959.

- Ross, W.J., Second-order effects in high-frequency transionospheric propagation, J. Geophys. Res., 70, 597, 1965.
- Smith III, F.L., Determination of rates of production and loss of electrons in the F region of the ionosphere from observations of geostationary satellite transmissions, <u>Tech. Rept. SEL-67-102</u>, Radioscience Lab., Stanford Electronics Lab., Stanford University, Stanford, California, March 1968.
- Smith, D.H., Diurnal variation of the mean Faraday factor at Arecibo, J. Geophys. Res., 75, 823, 1970.
- Taylor, H.A., Jr., H.C. Brinton and M.W. Pharo, III, Contraction of the plasmasphere during geomagnetically disturbed periods, <u>J. Geophys. Res.</u>, 73, 961, 1968.
- Yeh, K.C. and V.H. Gonzalez, Note on the geometry of the Earth magnetic field useful to Faraday effect experiments, <u>J. Geophys. Res.</u>, <u>65</u>, 3209, 1960.
- Yoh, P., Diurnal variation of the electron concentration in the lower magnetosphere as detected by lunar radar experiment, <u>J. Geophys. Res.</u>, 73, 253, 1968.